Annu. Rev. Biomed. Data Sci. 2021. 4:417–47

First published as a Review in Advance on June 1, 2021

The *Annual Review of Biomedical Data Science* is online at biodatasci.annualreviews.org

https://doi.org/10.1146/annurev-biodatasci-110920-093120

Annual Review of Biomedical Data Science

Satellite Monitoring for Air Quality and Health

Tracey Holloway,[1,2] Daegan Miller,[1] Susan Anenberg,[3] Minghui Diao,[4] Bryan Duncan,[5] Arlene M. Fiore,[6] Daven K. Henze,[7] Jeremy Hess,[8] Patrick L. Kinney,[9] Yang Liu,[10] Jessica L. Neu,[11] Susan M. O'Neill,[12] M. Talat Odman,[13] R. Bradley Pierce,[2,14] Armistead G. Russell,[13] Daniel Tong,[15] J. Jason West,[16] and Mark A. Zondlo[17]

[1]Nelson Institute Center for Sustainability and the Global Environment, University of Wisconsin–Madison, Madison, Wisconsin 53726, USA; email: taholloway@wisc.edu

[2]Department of Atmospheric and Oceanic Sciences, University of Wisconsin–Madison, Madison, Wisconsin 53726, USA

[3]Department of Environmental and Occupational Health, George Washington University, Washington, DC 20052, USA

[4]Department of Meteorology and Climate Science, San José State University, San Jose, California 95192, USA

[5]Atmospheric Chemistry and Dynamics Laboratory, NASA Goddard Space Flight Center, Greenbelt, Maryland 20771, USA

[6]Lamont-Doherty Earth Observatory and Department of Earth and Environmental Sciences, Columbia University, Palisades, New York 10964, USA

[7]Department of Mechanical Engineering, University of Colorado, Boulder, Colorado 80309, USA

[8]Department of Environmental and Occupational Health Sciences, Department of Global Health, and Department of Emergency Medicine, University of Washington, Seattle, Washington 98105, USA

[9]School of Public Health, Boston University, Boston, Massachusetts 02215, USA

[10]Gangarosa Department of Environment Health, Rollins School of Public Health, Emory University, Atlanta, Georgia 30322, USA

[11]Jet Propulsion Laboratory, California Institute of Technology, Pasadena, California 91109, USA

[12]Pacific Northwest Research Station, USDA Forest Service, Seattle, Washington 98103, USA

[13]School of Civil and Environmental Engineering, Georgia Institute of Technology, Atlanta, Georgia 30332, USA

[14]Space Science and Engineering Center, University of Wisconsin–Madison, Madison, Wisconsin 53726, USA

[15]Atmospheric, Oceanic and Earth Sciences Department, George Mason University, Fairfax, Virginia 22030, USA

[16]Gillings School of Global Public Health, University of North Carolina, Chapel Hill, North Carolina 27599, USA

[17]Department of Civil and Environmental Engineering, Princeton University, Princeton, New Jersey 08544, USA

Keywords

satellites, air quality, public health, $PM_{2.5}$, ozone, health impacts

Abstract

Data from satellite instruments provide estimates of gas and particle levels relevant to human health, even pollutants invisible to the human eye. However, the successful interpretation of satellite data requires an understanding of how satellites relate to other data sources, as well as factors affecting their application to health challenges. Drawing from the expertise and experience of the 2016–2020 NASA HAQAST (Health and Air Quality Applied Sciences Team), we present a review of satellite data for air quality and health applications. We include a discussion of satellite data for epidemiological studies and health impact assessments, as well as the use of satellite data to evaluate air quality trends, support air quality regulation, characterize smoke from wildfires, and quantify emission sources. The primary advantage of satellite data compared to in situ measurements, e.g., from air quality monitoring stations, is their spatial coverage. Satellite data can reveal where pollution levels are highest around the world, how levels have changed over daily to decadal periods, and where pollutants are transported from urban to global scales. To date, air quality and health applications have primarily utilized satellite observations and satellite-derived products relevant to near-surface particulate matter <2.5 μm in diameter ($PM_{2.5}$) and nitrogen dioxide (NO_2). Health and air quality communities have grown increasingly engaged in the use of satellite data, and this trend is expected to continue. From health researchers to air quality managers, and from global applications to community impacts, satellite data are transforming the way air pollution exposure is evaluated.

1. INTRODUCTION

Over the past decade, satellite data have increasingly been applied to public health and air quality analyses. These applications have been supported by investments into Earth-observing satellites, as well as initiatives to spur effective utilization of satellite data by the health and air quality communities. While health-relevant, near-surface concentrations of pollutants may be inferred from some satellite data products, the successful interpretation of satellite data for health exposure requires an understanding of the strengths and limitations of satellite data. In particular, health applications require linking satellite data to surface-level air quality concerns.

This review presents an overview of satellite data applications to health and air quality issues, with a variety of recent examples. These insights draw from the work of the NASA HAQAST (Health and Air Quality Applied Sciences Team), a four-year applied research initiative working to connect NASA resources and expertise with stakeholders in the air quality and public health communities (1). The authors of this review are all members and project leaders of the 2016–2020 HAQAST, and present here an overview of key ideas in linking satellite data with air quality and health. (For information on the current HAQAST team, funded from 2021 to 2025, the reader is invited to visit **https://HAQAST.org**).

The strengths and limitations of satellite data are best understood in the context of air quality data more broadly. Three main data sources may be used to characterize ambient concentrations of air quality: in situ measurements, computer models, and remote sensing platforms like satellites. The temporal and spatial scale of analysis fundamentally affects the utility of air quality data, as does the pollutant of interest. The appropriateness of air quality data products for time and space scales is shown in **Figure 1** (2).

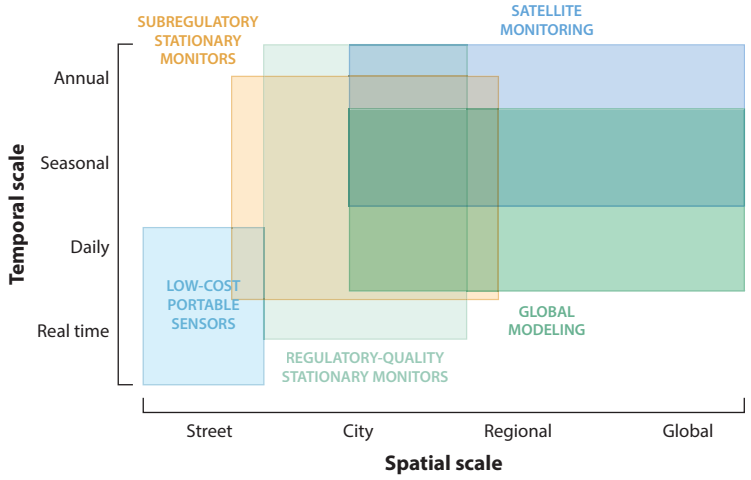

Figure 1

Illustrative summary of general abilities of air pollution monitoring technologies by effective spatial and temporal scales to provide air quality information. Figure adapted with permission from Reference 2; copyright 2019 American Thoracic Society.

Stationary monitors represent the most widely used source of air quality information in most developed countries. These monitors are often considered the gold standard for air quality information and have been widely used for epidemiologic studies. However, ground-based monitors are limited in their geographic coverage, due both to their initial expense and to the cost of maintaining a network. As such, they are typically sited to capture air pollution in urban areas, with less coverage in rural areas. For example, the United States has thousands of monitors for ground-level ozone and particulate matter <2.5 μm in diameter ($PM_{2.5}$), although approximately 80% of U.S. counties lack even a single monitor (3). This lack of spatial coverage limits the evaluation of rural exposure to air pollution and impedes the evaluation of nonurban emission sources, from agriculture to forest fires. These spatial biases limit air pollution exposure data available to assess health impacts over a wide area.

Around the world, many countries have little or no publicly available monitoring data, even for common pollutants. Recently, 141 countries were found to have no regular $PM_{2.5}$ monitoring at all, and only 23 nations have more than three monitors per million inhabitants (4). Shaddick et al. have estimated that 92% of the world's population lives in areas exceeding World Health Organization guidelines for $PM_{2.5}$ (5). People living in low- and middle-income countries are disproportionately burdened with the mortality associated with outdoor air pollution, and the annual number of deaths is projected to more than double by 2060 (6). de Sherbinin et al. have highlighted the potential for properly constructed satellite-based indicators to inform global air pollution levels for decision-making and public outreach (7).

The primary advantage of satellite data is their high spatial coverage, bridging spatial gaps in current ground-based networks. Satellite data show us where pollution levels are highest around the world, how those levels are changing over the last few decades, and where pollution is transported downwind, including over regional and intercontinental distances. Although many satellite data products may be used to assess year-to-year change, challenges occur in connecting satellite trends to those at the surface and—for some instruments and retrievals—in accounting for changes in instrument functionality over the years.

The most significant constraint of satellite data for health applications is the lack of surface-level information. Satellite data typically report chemical abundance in the column of air above the earth, and additional analysis steps are required to link these columns with air quality on the ground. Most satellites that detect air pollution are polar orbiting, also known as satellites in low-Earth orbit. These satellites pass over the poles of the earth and provide data over most of the world every day, or every few days. While these satellites provide global coverage, they offer just one or two snapshots a day (or less, depending on the instrument design, orbit, cloud cover, and land cover). Recent and upcoming geostationary satellites observing air quality offer the potential for greater temporal data coverage. Geostationary satellites orbit with the earth, so they are able to provide data over a particular geographic region at hourly or better frequencies during daylight hours (8). Depending on the instrument and chemical retrieval, the spatial resolution of satellite data varies from ∼1 to ∼50 km. Only a few health-relevant pollutants in the atmosphere may be reliably detected from space, and even these vary in data quality and spatial resolution.

Satellite-based estimates of $PM_{2.5}$ have emerged as some of the most important tools for health assessment, while also some of the most complex applications of satellite data. Concentrations of $PM_{2.5}$ cannot be directly observed from satellites, but rather inferred using models or monitoring data. Rather than detecting $PM_{2.5}$ directly, satellites measure aerosol optical depth (AOD) and other markers of particulate loading in the atmosphere. AOD is a unitless measure of light absorption by particles in the atmosphere, dependent on the total mass of particles in the atmosphere, the size and chemical characteristics of the particles, the vertical distribution of particles the atmosphere, and other factors. As a result, the relationship between columnal AOD and surface $PM_{2.5}$ varies in space and time.

Combining ground monitors with satellite or modeling data can significantly enhance the spatial coverage of the derived $PM_{2.5}$ data, providing continuous datasets in space and time (e.g., 5, 9, 10). Over the years, various methods have been used for deriving this relationship, such as linear regression models (11–13), multiple regression models, or generalized additive models (14–17), as well as more advanced data fusion (18) and machine learning (ML) approaches (19). Compared with parametric regression models, ML algorithms have more relaxed requirements on the independence of observations and collinearity among predictor variables. ML algorithms can also more efficiently handle massive datasets, nonlinear relationships, and interactions among predictors than statistical models. A few widely used ML algorithms include decision tree–based models such as random forest (20–25), gradient boosting (26), neural networks (12), and deep learning (27, 28), as well as ensemble models integrating multiple ML algorithms (29, 30). The temporal resolution of these models ranges from daily to monthly, the study period ranges from several months to multiple years, and the spatial scale ranges from subregional to national. When used to estimate ambient $PM_{2.5}$ concentrations, two recent comparison studies indicated that ML algorithms can often outperform chemical transport models (CTMs) and traditional statistical models such as kriging and multivariate regression, with cross-validation R^2 values exceeding 0.8 when compared with ground observations (31, 32). However, one study with a specific focus on models' spatiotemporal predictive capabilities (comparing models developed using the same set of input data sources) found that statistical models accounting for spatial dependence, such as the downscaler, outperform any other method (33). The underperformance of ML algorithms such as random forest and neural networks might be due to the smaller number of predictors included in this comparison than in typical applications of these methods and the fact that these ML methods do not account explicitly for the spatial dependence of $PM_{2.5}$.

Various ancillary data may be included for improving the relationship function, such as temperature, relative humidity, wind field, land use, and road density. Satellite-derived $PM_{2.5}$ can be further evaluated against ground monitor data, optimizing the AOD–$PM_{2.5}$

relationship for various locations. One example is SPARTAN (Surface Particulate Matter Network; **https://www.spartan-network.org**), which provides public datasets for satellite data evaluation (34). Aircraft data can also support the linking of satellite columns and surface $PM_{2.5}$ abundance, including from flight campaigns designed to support air quality analysis (e.g., 35).

Past review articles have outlined the opportunities and challenges in applying satellite data for air quality (8), for evaluating emission inventories (36), and for estimating near-surface $PM_{2.5}$ (10). Here we expand on this body of work to focus on health applications of satellite-derived air quality data, including a discussion of satellite data for epidemiological studies (Section 2) and health impact assessments (Section 3); air quality trends (Section 4); air quality regulation (Section 5); and smoke from wildfires, prescribed burns (PBs) (Section 6), and other emissions sources (Section 7). We conclude with an overview of satellite capabilities and limitations (Section 8).

2. SATELLITE DATA FOR EPIDEMIOLOGICAL STUDIES

Epidemiological studies for air pollution analyze associations between exposure to airborne contaminants and health outcomes, controlling for confounding factors, to isolate and quantify relationships between the concentration of a pollutant and associated health risks. A growing body of epidemiological research at regional to continental scales has used satellite-derived exposure data to quantify health risks of $PM_{2.5}$ and NO_2. Past satellite missions were not designed with health analysis in mind, but research connecting remote sensing and epidemiology has highlighted the opportunities to leverage existing data for new health applications. These successes motivate the development of MAIA (Multi-Angle Imager for Aerosols), an upcoming instrument from NASA explicitly designed to quantify the health impacts of different types of air pollution.

Satellite-derived $PM_{2.5}$ exposure estimates enable air pollution evaluation in areas where monitors are sparse or nonexistent. Using space-based measurements can improve estimation of spatiotemporal changes in $PM_{2.5}$ to support improved understanding of health response to pollution exposure. For example, Strickland et al. reported significant associations between satellite-derived daily $PM_{2.5}$ exposure and emergency room visits for several pediatric conditions, including asthma or wheeze and upper respiratory infections, in the U.S. state of Georgia (37). Combining satellite remote sensing data and CTM simulations, Stowell et al. estimated the associations between cardiorespiratory acute events and exposure to smoke $PM_{2.5}$ in Colorado and found statistically significant associations for asthma [odds ratio (OR) = 1.081] and combined respiratory disease (OR = 1.021) for an increase in fire smoke $PM_{2.5}$ of 1 $\mu g/m^3$ (38; see also 39). Xiao et al. examined the associations between maternal $PM_{2.5}$ exposure and adverse birth outcomes using three exposure assessment methods and found that health effects calculated using gap-filled satellite $PM_{2.5}$ had similar magnitudes to those using central-site measurements, but with narrower confidence intervals due to reduced exposure error (40). At the national scales, satellite-derived short-term increase in $PM_{2.5}$ exposure has been associated with an increase in daily mortality in the Medicare population in the United States, and long-term average $PM_{2.5}$ exposure has been positively linked to elevated risk of cardiovascular disease and incident stroke among Chinese adults (41–43).

Satellite-derived $PM_{2.5}$ is becoming an important tool to advance air pollution health effects research in developing countries with sparse ground monitoring networks. For example, Tapia et al. reported that satellite-derived $PM_{2.5}$ exposure was associated with adverse pregnancy outcomes, cardiorespiratory emergency room visits, and daily cardiorespiratory mortality, especially among older people, in Lima, Peru (44–46). Heft-Neal et al. reported that an increase of 10 $\mu g/m^3$ in $PM_{2.5}$ concentration is associated with a 9% rise in infant mortality in sub-Saharan Africa,

suggesting a doubling of previous estimates of global deaths of infants that are associated with air pollution (47).

Satellite observations have also been instrumental in estimates of health effects of NO_2 (48). As with other pollutants, NO_2 from satellites can enable air pollution evaluation in areas where monitors are sparse or nonexistent. While the satellite detects the column of NO_2 abundance rather than surface concentrations, studies have found a correlation in spatial and temporal patterns between column and surface NO_2 (49, 50). NO_2 concentrations are highly spatially variable, with concentrations that decline to urban background levels at a distance greater than 300–500 m from major roadways (51). Further, asthma development may be more strongly associated with intraurban variation in NO_2 concentrations than with urban-rural variation (52, 53). Therefore, for NO_2, very high spatial resolution concentration estimates (100 m to 1 km) are desirable for epidemiological analysis. Exposure assessment methods using satellite data combined with techniques such as land use regression modeling are increasingly able to predict NO_2 concentrations at these fine spatial scales (54). With higher spatial resolutions available from recent and upcoming satellites, assessing NO_2 exposure for epidemiological analysis is rapidly advancing in availability and accuracy.

Common sources that contribute to $PM_{2.5}$, both emitted directly and formed chemically, include the combustion of fossil fuels, biomass burning (both PBs and wildfires), and biogenic emissions such as from forests, agricultural soils, and the ocean. These sources produce a complex mix of reactive sulfur, nitrogen, and carbon that create ozone and $PM_{2.5}$, with strong spatial and temporal variations in their relative importance. The upcoming MAIA mission from NASA is designed to support future epidemiological studies on the relative toxicity of these different particulate matter (PM) components. As the first NASA mission designed explicitly for public health analysis, MAIA builds upon the legacy of MISR (Multi-Angle Imaging SpectroRadiometer). MAIA will have the capability to inform the chemical speciation of $PM_{2.5}$ to support species-specific health assessments. The MISR instrument defines a set of aerosol mixtures to represent aerosol types around the world representing the major ambient particle species. MISR-retrieved aerosol properties have been successfully used as predictors of major $PM_{2.5}$ species such as sulfate, nitrate, organic carbon (OC), and elemental carbon (EC) (55–58). The upcoming MAIA instrument is similarly designed to combine multispectral, polarimetric, and multiangular capabilities into an imaging system capable of mapping total and speciated PM at neighborhood scale over a selected set of urban centers around the world (59, 60). Over the primary target areas, MAIA's sampling frequency will be three to four times per week. In addition to various aerosol optical properties, the MAIA research team will combine satellite data and models to generate ground-level daily $PM_{2.5}$ sulfate, nitrate, OC, EC, and dust concentrations at 1-km spatial resolution. MAIA is being coordinated with planned epidemiological studies to help determine the relative toxicity of various PM components and to assess the effects of particle size and composition on adverse birth outcomes, cardiovascular and respiratory disease, and premature death.

3. SATELLITE DATA AND HEALTH IMPACT ASSESSMENTS

Health impact assessment (or risk assessment) is a process for estimating the burden of disease attributable to air pollution in a given population. These studies combine concentration–response functions from epidemiological studies with estimates of population exposure to air pollutants. Health risk assessments may also be used to estimate the changes in the disease burden under different exposure conditions (e.g., future climate change or emissions policy implementation). A key challenge for air pollution health impact assessments, from local to global scales, is the need for measurements or model predictions of air pollutant concentrations that are high quality,

standardized, and continuous over long periods, with sufficiently high spatial resolution to capture variability commensurate with population gradients. Increasingly, satellite remote sensing data are being used in combination with in situ monitors and CTM, through data fusion or other methods, to estimate air pollution–related health impacts.

Satellite-derived estimates of surface-level $PM_{2.5}$ concentrations have been incorporated into a variety of health impact assessments that use the high spatial resolution, broad spatial coverage, and year-to-year availability that are intrinsic to these datasets. Remote sensing–based estimates of exposure from van Donkelaar et al. (61) were used by Evans et al. (62) to estimate the global premature deaths associated with long-term exposure to $PM_{2.5}$. This type of satellite-informed data product has become a standard component of global scale estimates of $PM_{2.5}$ health impacts that are updated annually (63). Satellite-derived data, often resolved at the 1- to 10-km scale, have been used to downscale coarser global model calculations of $PM_{2.5}$ in order to better capture sharp gradients in population distributions. This approach increases the ability of global models to inform health impacts from individual $PM_{2.5}$ sources, sectors, or future emission scenarios (see **Figure 2**) (64–67).

Recent assessments have highlighted the potential for satellite data to inform public health risks from ambient air pollution. Satellite-derived $PM_{2.5}$ from Dalhousie University (9, 10, 68, 69) were used for global estimates of $PM_{2.5}$ in the 2017 Global Burden of Disease study (GBD) and other studies (70). The GBD health burden estimates are derived using health impact assessment methods, which combine information on exposure-response functions (ERFs) for specific diseases and causes of death, baseline rates of those health outcomes, estimates of ambient air pollution concentrations, and the numbers of people exposed. The $PM_{2.5}$ ERFs used by the GBD study are based on integrating ERFs from a range of epidemiologic literatures, including those of ambient air pollution, household air pollution, second hand smoking, and active smoking (71). The GBD assumes that particle toxicity is independent of PM source type and depends only on concentration, consistent with the bulk of the epidemiological evidence for premature mortality risk due to long-term $PM_{2.5}$ exposure.

The widely varying $PM_{2.5}$ exposure levels around the world pose a challenge in estimating global impacts of $PM_{2.5}$. Risk estimates used in the GBD drew primarily from cohort studies in the United States and Europe, where $PM_{2.5}$ concentrations seldom exceed 25 ug/m^3 on an annual average. Recently, however, new cohort studies have emerged from China, and over time, it can be anticipated that relevant studies will be published from India and other countries where concentrations range up to 100 ug/m^3 and beyond, thus providing empirical information on the ERF in a range that, until now, has only been estimated (72, 73). In fact, one study focusing on the ERF at high concentrations estimated 8.9 (7.5–10.3) million deaths globally from $PM_{2.5}$ in 2015 (71), which is markedly higher than GBD 2017's estimate of 2.9 (2.5–3.4) million (70).

High-quality satellite-derived estimates of $PM_{2.5}$ have only been produced in the past decade, which has raised awareness of ambient air pollution as an issue that spans the local and the global scales (74, 75). While air quality has improved over the past few decades in, for example, the United States and western Europe, driven primarily by clean air regulations, pollutant concentrations in China have increased markedly and have likely peaked and then declined in recent years (76–78). In contrast, concentrations continue to grow and are expected to continue to worsen in, for example, India and Africa (79).

Fewer health impact assessments have focused on NO_2, despite the growing utilization of satellite-detected NO_2 for other air quality applications. An example of a global NO_2 health impact assessment has found that traffic-related NO_2 exposure has been associated with approximately four million pediatric asthma cases globally each year, about 13% of the global asthma burden (80). This percentage ranged up to 48% in urban areas, where NO_2 is highest. NO_2

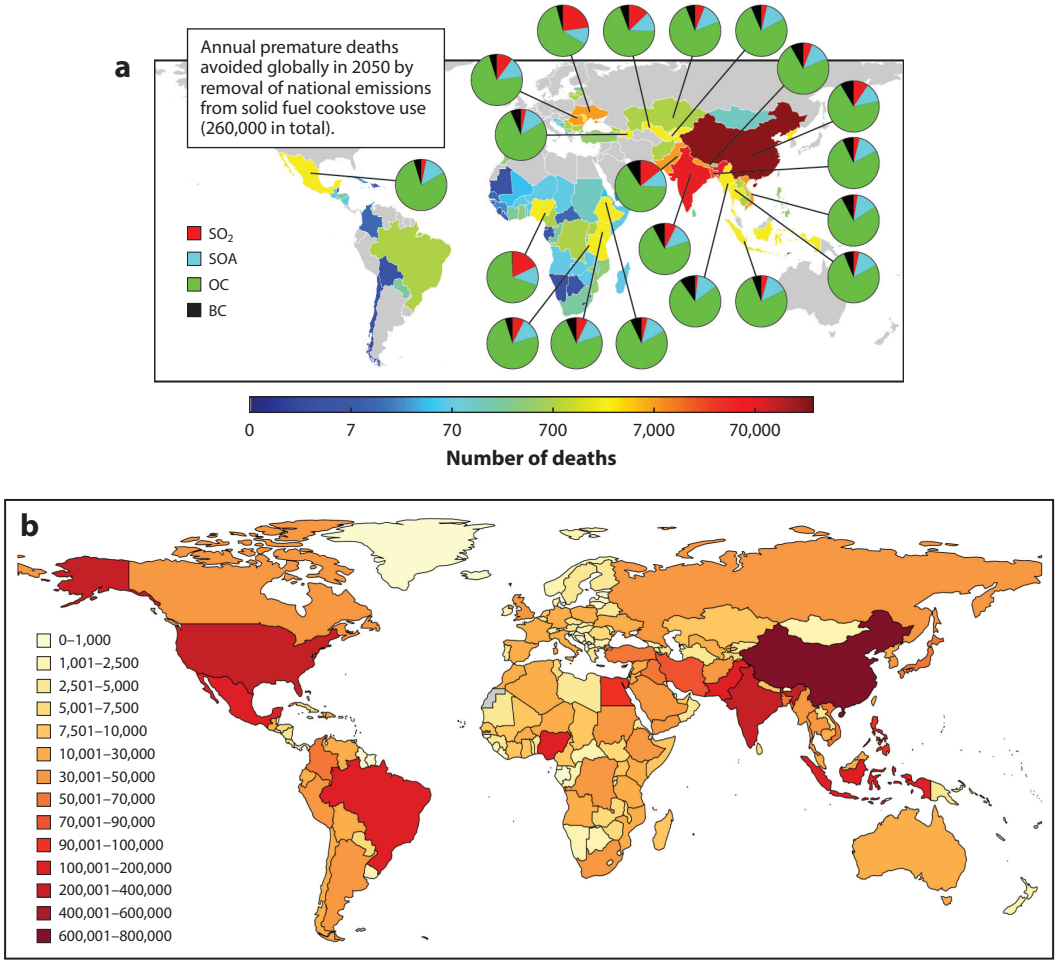

Figure 2

(*a*) Model simulations in Reference 67 conducted at 2° × 2.5° used to estimate $PM_{2.5}$ health impacts owing to emissions from particular species and countries, with satellite-derived $PM_{2.5}$ estimates used to downscale the simulation results to 0.1° × 0.1° resolution. Panel adapted with permission from Reference 67; copyright 2017 the authors. (*b*) Number of new pediatric asthma cases in each country due to NO_2 exposure in 2011. Panel adapted with permission from Reference 80; copyright 2019 the authors. Abbreviations: BC, black carbon; NO_2, nitrogen dioxide; OC, organic carbon; $PM_{2.5}$, particulate matter <2.5 μm in diameter; SO_2, sulfur dioxide; SOA, secondary organic aerosol.

exposure and pediatric asthma incidence is now under consideration for inclusion in the GBD study, where satellite data would be a key input for exposure assessment. If this risk–outcome pair is included, it would complement the current estimates of $PM_{2.5}$- and ozone-attributable mortality burdens, and it would provide a fuller accounting of the health damages from ambient air pollution worldwide (70).

4. SATELLITE DATA AND AIR QUALITY TRENDS

Satellite data show that pollution levels in urban areas typically change slowly over time (i.e., years), although the construction of power plants or the implementation of emission controls

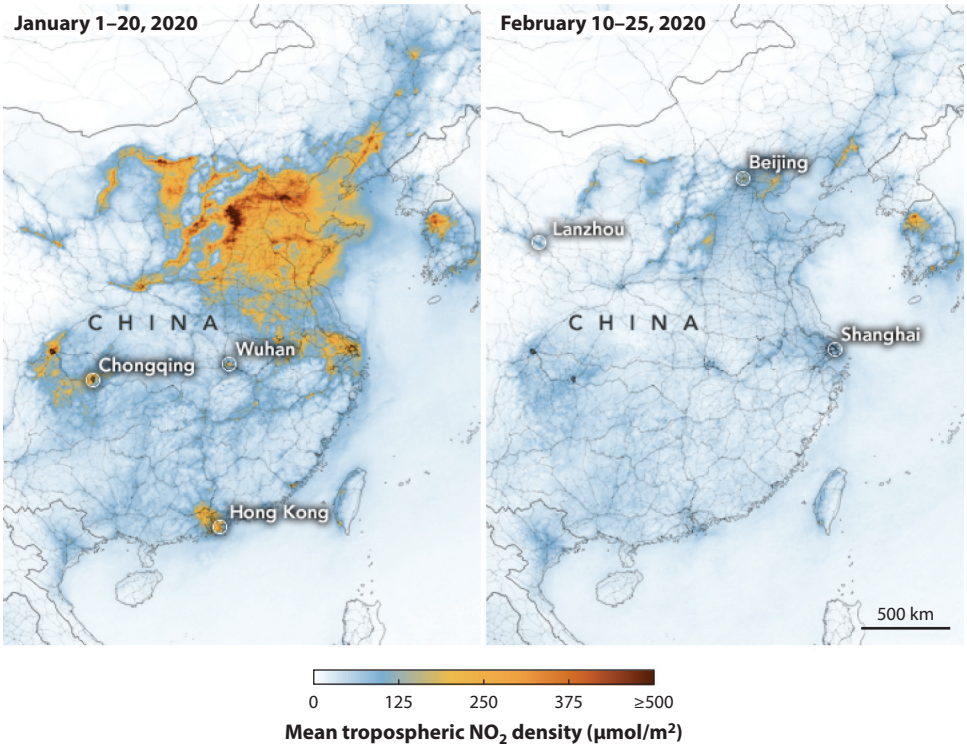

Figure 3

Nitrogen dioxide (NO_2) columns over eastern China in January 2020 (*left*) and February 2020 (*right*) retrieved from the Ozone Monitoring Instrument (OMI) aboard the Aura satellite. Changes reflect reduced economic activity in response to the COVID-19 (coronavirus disease 2019) pandemic. Images courtesy of NASA (**https://airquality.gsfc.nasa.gov/news/airborne-nitrogen-dioxide-plummets-overchina**).

on power plants can rapidly change pollutant levels (81). Records from the Ozone Monitoring Instrument (OMI) aboard the Aura satellite indicate that urban NO_2 levels have decreased by 20–60% over much of the United States and Western Europe since 2005 and over China since about 2011. These trends are due to emission controls on power plants and transportation. In contrast, economic growth in many tropical and subtropical countries has led to increased pollution levels over this same period (82–84).

Satellite data indicate that the recent lockdowns associated with the COVID-19 (coronavirus disease 2019) pandemic have led to decreases in many pollutants over several months in the boreal winter and spring of 2020 (see **Figure 3**). In Chinese cities, NO_2 columns decreased 40% relative to the same time in the previous year, with somewhat lower reductions (20–38%) in the United States and Western Europe (85). However, understanding the changes in air quality resulting from these emissions reductions requires considering the time of year at which the reductions occurred, the background pollution levels in the region, and the role of weather in both photochemical production and the removal of pollutants through precipitation.

While satellites cannot yet measure ozone directly at the surface, they can provide valuable information on ozone in the mid-troposphere (6). Ozone is not emitted directly but is produced from precursor gases such as nitrogen oxides ($NO_x = NO + NO_2$) and volatile organic compounds (VOCs) that react in the presence of sunlight. Satellite measurements of NO_2 and formaldehyde

(HCHO), an indicator of reactive VOCs, provide an indicator of chemical regime and a valuable resource for evaluating and improving the models used for understanding the sources of ozone. As emissions decline in some parts of the world and continue to increase in others, the mixture of ozone sources at a given location will change with time (86).

Air quality data from satellites, including for trend analysis, bear relevance to a range of policy and regulatory issues. Currently, the U.S. Environmental Protection Agency (EPA) National Ambient Air Quality Standards (NAAQS) only consider ground-based monitor data when determining compliance with the standards, although in a recent evaluation of compliance with the sulfur dioxide (SO_2) standard, models were used in the absence of monitors to evaluate NAAQS compliance. While the U.S. regulatory framework is tied directly to ground-based monitoring networks, satellite data are playing a growing role in providing evidence of spatial and temporal trends in atmospheric pollutant transport, chemistry, and emissions. The air pollution regulatory process recognizes the potential for natural sources to affect compliance with air quality standards and thus includes mechanisms to screen out high-pollution events that are not caused by regulated emissions. Source attribution is required for all high-pollution events, as the specific mechanisms depend on the source type (for example, pollution produced from natural sources versus transport of pollution produced from international anthropogenic emissions).

Because satellite measurements intrinsically sample the column of air above Earth's surface, direct comparisons to air quality stations operated near the surface remain challenging. However, the spatial coverage of satellite data complement ground-based networks to support policy applications. For example, long-term satellite records provide clear evidence for the success of air quality regulations at reducing two trace gases, SO_2 (as shown in **Figure 4**) and NO_2. Each of these is associated with direct health impacts and contributes to chemically formed pollution: SO_2 contributes to sulfate PM and NO_2 contributes to both to ozone and to nitrate PM. In addition to interannual trends, satellites can detect trends for species that have strong seasonal emissions. **Figure 5** shows the highly varying seasonal patterns of NH_3, another precursor of sulfate and nitrate aerosols, due to agricultural emissions from crop fertilization and livestock waste. Despite its importance in $PM_{2.5}$, NH_3 is not regulated in the Clean Air Act in part due to a lack of observational constraints on emissions and concentrations. Satellite NH_3 measurements are helping to guide the placement of future sites in ground-based networks for quantifying nitrogen deposition (87) and constraining emissions (88). Numerous satellite instruments also detect HCHO, a useful indicator for chemical reactions involving VOCs that lead to ozone and organic aerosol formation (89). During the warm season over the United States, the dominant HCHO source is isoprene, a biogenic VOC emitted from vegetation. New techniques show promise for direct retrieval of isoprene, which, together with HCHO, will provide important constraints on the atmospheric chemistry of ozone and haze formation (90). In summary, a growing portfolio of satellite data products can be applied to improve both the spatial and temporal aspects of emission inventories, as well as to provide key insights regarding atmospheric processes affecting health-relevant pollutants.

Satellite data are now incorporated in some aspects of U.S. air quality policy implementation, and we give some brief examples of these applications here. The annual U.S. EPA air quality trends report now includes long-term changes in tropospheric column NO_2 observed from space (91). Under the NAAQS, states with counties out of compliance with a standard are required to submit a state implementation plan (SIP) that describes an approach to attaining the standard. Satellite NO_2 data have been featured in SIPs submitted by the state of Texas for declining levels of NO_x, a key precursor to ozone formation, and satellite NO_2 and HCHO data have been used by the state of Connecticut as weight-of-evidence for photochemical conditions shaping regional high-ozone events (92–94). Satellite data have been applied to identify episodic, high-pollution events

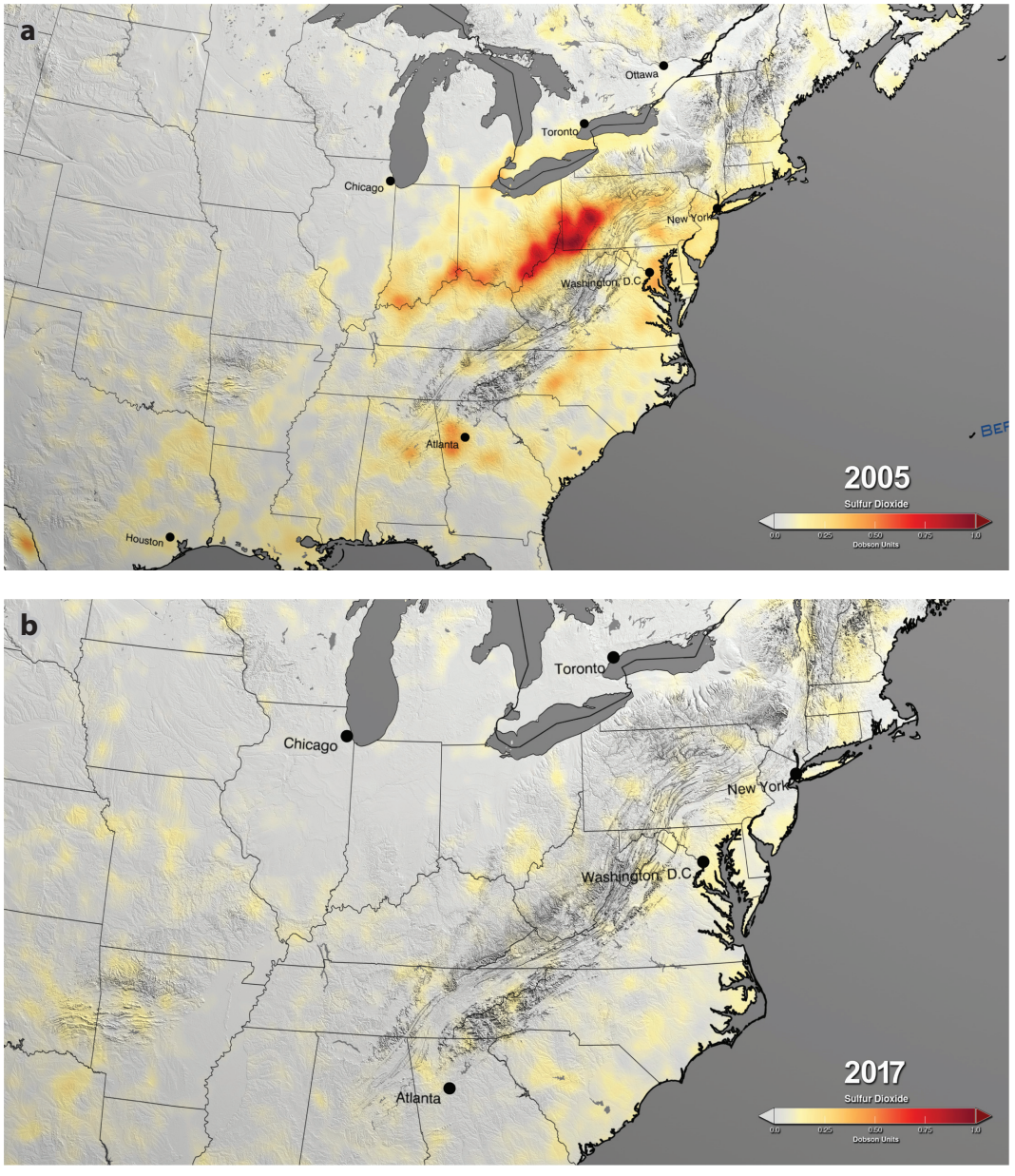

Figure 4

Sulfur dioxide (SO_2) columns over the eastern United States in 2005 (*a*) and in 2017 (*b*) retrieved from the Ozone Monitoring Instrument (OMI) aboard the Aura satellite. Changes reflect technologies, policies, and fuel use changes. Images courtesy of NASA (**https://airquality.gsfc.nasa.gov/particulate-matter**).

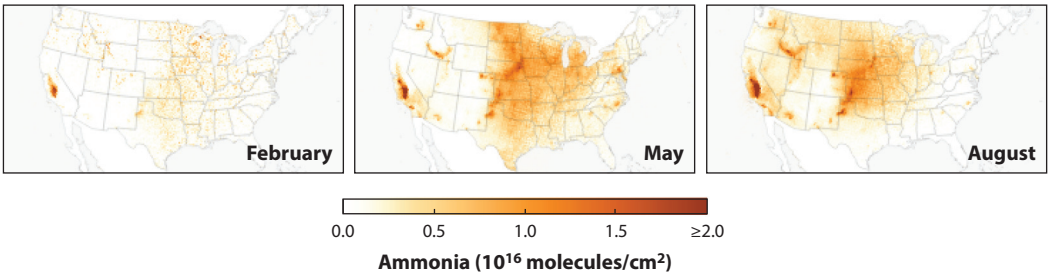

Figure 5

Ammonia (NH_3) columns over the United States in 2016 for February (*left*), May (*middle*), and August (*right*), showing increased agricultural emissions from crop fertilization and animal waste. Data retrieved from the infrared atmospheric sounding interferometer instruments onboard the MetOp satellites. Images courtesy of NASA (**https://earthobservatory.nasa.gov/images/144351/the-seasonal-rhythms-of-ammonia**).

from sources such as wildfires, dust, and even fertilizer application in agricultural regions, often in combination with models and ground-based measurements. More specifically, multiple satellite products have been used in exceptional event demonstrations that make a case for excluding these events from counting toward noncompliance with the ozone NAAQS by documenting a range of observations (weight of evidence) indicating that ozone enhancements were produced from transported wildfire plumes rather than anthropogenic emissions (95). Satellite products have also been used in combination with models and other observations to identify exceptional events associated with high-ozone air masses from the stratosphere into the lower troposphere, as well as international transport of ozone pollution (96).

5. SATELLITE DATA FOR WILDFIRE RESPONSE AND PRESCRIBED BURNS

In the United States, wildfires and PBs (collectively referred to as wildland fires) are becoming an ever-larger fraction of health-damaging air emissions. Remotely sensed data have a wide variety of applications to both PB and wildfire operations, giving information about the atmospheric aerosol loading, trace gases emitted from fires, and especially where the fires are occurring via satellite fire detections (97). While fires are a natural part of many of our ecosystems, smoke from wildland fires is a significant health issue (98–102). $PM_{2.5}$ levels during fires can rise to levels of thousands of micrograms per cubic meter, and ozone levels can rise by tens of parts per billion, even on days outside of the ozone season (103, 104). For both pollutants, the resulting levels routinely exceed the U.S. NAAQS, and states are identifying cases where fires have led to high levels as part of their air quality planning activities (e.g., as part of exceptional event demonstrations) (105).

Satellite data products inform us about where the fires are occurring and horizontal and vertical transport patterns so that we can protect ourselves from the smoke with the aid of smoke forecasting systems and decision support programs such as the Interagency Wildland Fire Air Quality Response Program (106–111). Fundamental to such systems are the satellite fire detection products from the Moderate Resolution Imaging Spectroradiometer (MODIS), Visible Infrared Imaging Radiometer Suite (VIIRS), and Advanced Baseline Imager instruments aboard NASA and NOAA (National Oceanic and Atmospheric Administration) polar-orbiting and geostationary satellites. These instruments detect thermal anomalies across multiple wavelengths to determine a temperature and radiative energy per pixel, which are used to calculate a fire radiative power (FRP). The resolutions of these products range from 375 m to 4 km, with temporal resolutions of twice

daily to every 5 min. By detecting fires on the landscape we can then calculate PM emissions with FRP (e.g., the NASA Fire Energetics and Emissions Research) and estimate how high smoke is lofted into the atmosphere (112) using, for example, the FRP-based method by Sofiev et al. (113). These data also give insight into the seasonality and widespread occurrence of wildland fires. As new satellites are launched, new methods are being developed to aggregate satellite fire detections from multiple platforms using high–temporal resolution geostationary fire detection data to simulate timing of fire activity (a combination of fire front movement and internal perimeter burning) to allocate emissions hourly, simulating, for example, the explosive early-morning fire growth of the 2018 Camp wildfire (114). New methods are also available to statistically combine satellite observations, modeled concentrations, and ground measurements to provide best estimates of smoke concentrations during a wildfire event; this data fusion has been shown to better represent concentrations than any single source of concentration data (115).

Visible satellite imagery and AOD give information about the extent of plumes and the total loading of aerosols in the atmosphere. However, the vertical distribution of smoke is important, as it determines how much smoke is near the surface where people breathe. Instruments such as the CALIOPE (Cloud Aerosol Lidar with Orthogonal Polarization) satellite lidar system on the NASA CALIPSO (Cloud Aerosol Lidar and Infrared Pathfinder Satellite Observations) satellite help inform these questions by measuring vertically allocated backscattering along a narrow satellite path to provide a vertical distribution of particulates in the atmosphere (116). Other products such as MISR and the MAIAC (Multi-Angle Implementation of Atmospheric Correction) algorithm developed for MODIS estimate the height of the smoke plume's top (117, 118).

Air quality and health agencies, as well as technical specialists deployed with wildfire-fighting incident management teams, use the aforementioned smoke forecasting systems, surface monitoring data, and satellite products available through tools such as NASA Worldview to issue smoke forecasts and advisories to the public. One such product, the Smoke Outlook, is initialized with a statistical model based on surface observations, MODIS AOD, as well as meteorological parameters (119). The Smoke Outlook and other information are posted to smoke blogs such as the blog California Smoke Information (**http://californiasmokeinfo.blogspot.com/**), which gets millions of hits during periods of wildfire smoke impacts. The EPA also incorporates satellite fire detections and analyzed smoke plumes, along with surface monitoring data from permanent and temporary monitoring systems, to inform the public about current smoke and fire conditions in their Fire and Smoke Map (**https://fire.airnow.gov/**). Since satellite data products can be daunting to new users, we have developed two online 15-min training videos, "The Basics of Satellite Data for Smoke and Fire" and "NASA Worldview for Fire," to bring these important data to a new user community (**https://www.airfire.org/projects/haqast/2017NorthernCAWildfiresTT/training**).

PB of dead and live vegetation for agricultural, land clearing, or silvicultural purposes, or simply to reduce the wildfire risk, is the single largest source of primary PM in the Southeast United States (98). Most PB occurs in the late winter and early spring and is made up of many small (10–100 acres) fires (**Figure 6*b***). Individual fires can lead to locally high pollutant levels, and collectively they can lead to a substantial regional background of smoke-based pollution that has been associated with adverse health outcomes, potentially because PM from PBs shows an increased oxidative potential (103, 120–123). A growing air quality management concern is the expected increase in prescribed fire activity, in part to address the increasing risk of wildfires.

The ability to manage the location and time of PBs provides leverage to forest and air quality managers to reduce the adverse impacts of both prescribed and wildfire emissions, as PBs can be planned for places and times that minimize exposure. The Southern Integrated Prescribed Fire Information System (**https://sipc.ce.gatech.edu/SIPFIS/map/**) is a WebGIS (geographic

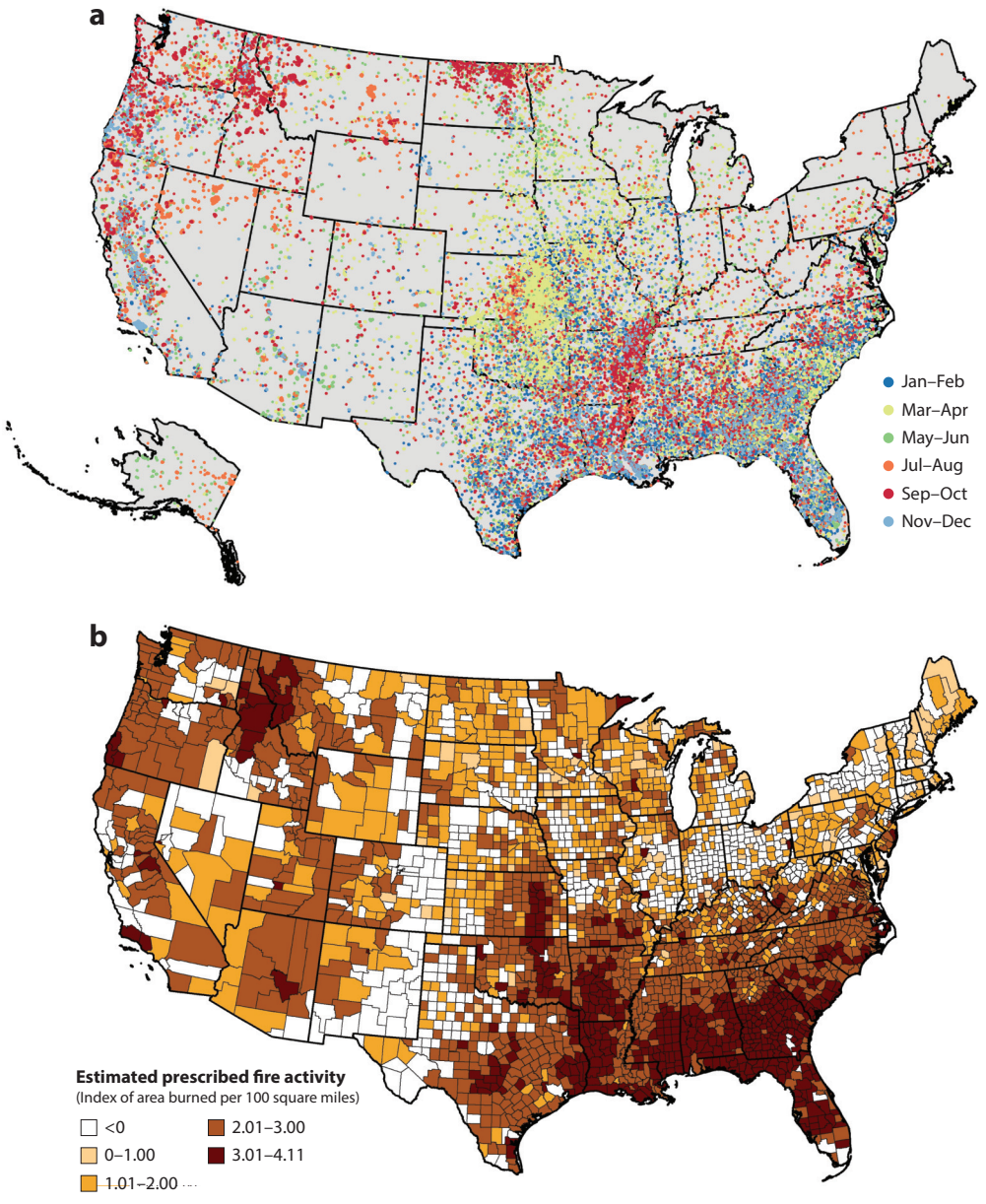

Figure 6

(*a*) 2017 MODIS (Moderate Resolution Imaging Spectroradiometer) fire hot spot detections color-coded by month. Panel adapted with permission from Reference 102. (*b*) Prescribed fire activity in the United States. Panel adapted with permission from **https://cohesivefire.nemac.org/node/63**.

information system)-based online analysis tool developed to provide predictions of the impacts of prescribed fire smoke on air quality and human health (111, 124, 125). Currently, its focus is on PB in the Southeast United States, although the air quality model domain covers the continental United States. The system uses a probabilistic, decision tree algorithm to predict the location

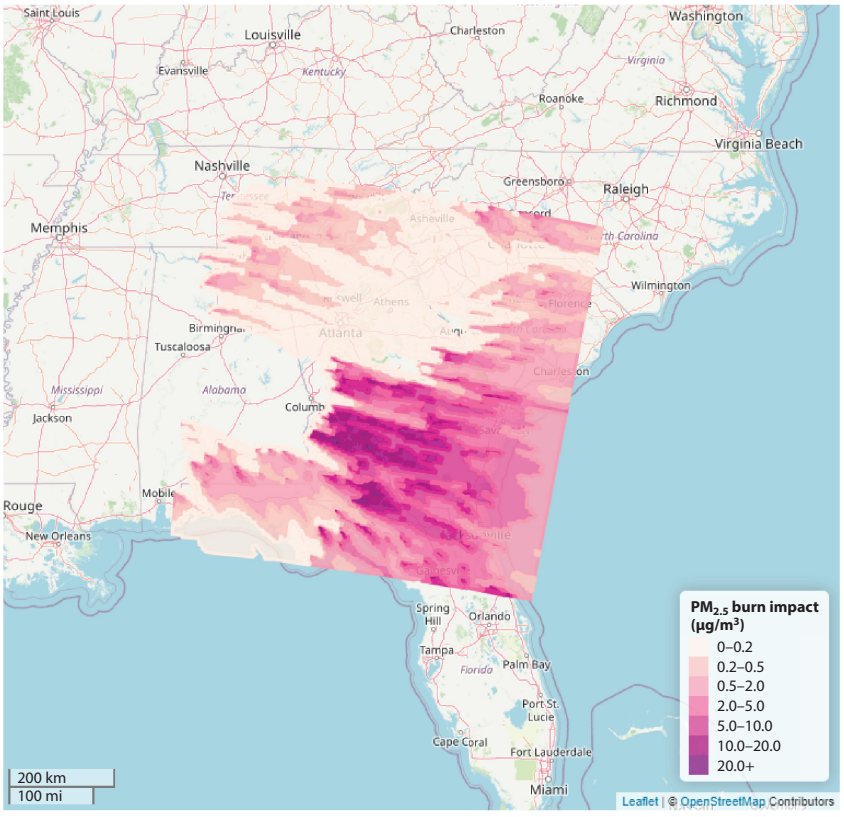

Figure 7

Prescribed burn impact forecast on January 25, 2020, by the Southern Integrated Prescribed Fire Information System (**https://sipc.ce.gatech.edu/SIPFIS/map/**). Abbreviation: $PM_{2.5}$, particulate matter <2.5 μm in diameter.

and size of PBs and is based in part on the Geostationary Operational Environmental Satellite (GOES), MODIS, and VIIRS retrievals of historic fire locations and sizes, as well as weather and forest conditions. Next, that information is fed into an air quality forecasting system called HiRes-X, which uses satellite observations to improve model simulations and forecast the likely impacts of PBs. (**Figure 7**). These forecasts are completed a day in advance to support forest and air quality managers' decisions about whether permits should be given, which are based in part on reducing human exposure. The HiRes-X system has been evaluated in part by low-cost sensors at schools and has been used for health studies by the US Forest Service and others (126).

6. SATELLITE DATA FOR DUST, AEROALLERGENS, AND SPECIALIZED SOURCES

Several other aerosols have impacts on human health and are amenable to remote sensing to support exposure assessments and related health applications. Progress on these activities depends on advances in sensing technology, the availability of ground observations, and priority applications, from exposure assessments to surveillance and early warning platforms. Dust and aeroallergens are two important examples that illustrate the opportunities and challenges of remote sensing for other specialized sources.

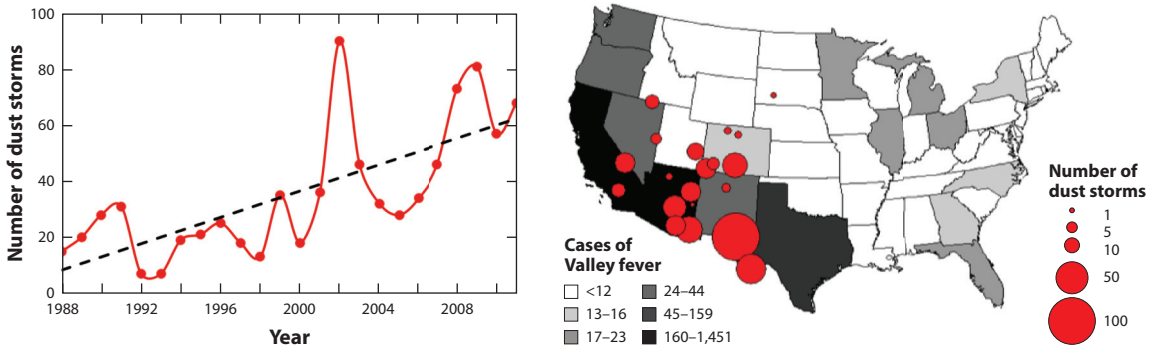

Figure 8

(*Left*) Frequency of dust storms increased at 12% per year between 1990 and 2011 in the United States. (*Right*) Dust storms (*red circles*) and Valley fever incidence (*gray shading*) in the United States. Map generated using data from Reference 130.

Dust storms are an air quality hazard that pose severe risks to public health and transportation safety in many parts of the world. Exposure to dust particles has been associated with a variety of adverse health effects, including cardiovascular mortality and heart attacks (127, 128). Dust storms also are associated with infectious diseases, such as meningitis in Africa and, in the Americas, *Coccidioidomycosis*, commonly known as Valley fever, an infection caused by inhalation of a soil-dwelling fungus (129, 130). Satellite observations are used to address several issues related to dust storms, such as reconstructing historical trends, identifying dust sources, and improving dust forecasts. For instance, Tong et al. (131) used the true color images of dust storms from the MODIS sensor aboard the Terra and Aqua satellites to train a dust detection algorithm and reconstructed long-term dust climatology over the western United States, which found that the frequency of locally originated windblown dust storms increased by 240% between 1990 and 2011 in the Southwest United States, which has high incidence rates of Valley fever infection (**Figure 8**) (130, 131).

The global remote sensing record has been widely used to identify active dust source areas (132–134). Satellite techniques and on-the-ground studies of soil and land cover characteristics of dust-emitting sites have clarified the relative frequency and intensity of dust emissions from different land use and soil types (133–135). Ginoux et al. (136) demonstrated the use of MODIS Deep Blue Level 2 (M-DB2) aerosol products to identify dust sources in West Africa. This approach identifies dust plumes by comparing dust optical depth (DOD) to a threshold value (136). An entry of DOD is found from the M-DB2 data if three criteria are met: (*a*) The angstrom wavelength exponent is negative ($\alpha < 0$), (*b*) the single-scattering albedo (ω) is smaller than 0.95, and (*c*) there is a positive difference in ω between 412 and 670 nm [$\omega(670) - \omega(412) > 0$]. If the determined DOD entry has a value smaller than 0.2, the satellite AOD record is considered a dust event. The abovementioned studies have revealed that dust is not emitted uniformly from across the landscape but is instead emitted from isolated hot spots in so-called preferential source areas by airborne plumes that coalesce so that a small fraction of the landscape comprises a majority of dust sources.

Aeroallergens, including pollens from wind-pollinated plants and fungal spores, are important environmental health exposures. Some pollens are highly allergenic, as are certain fungal spores. Exposure reliably leads to immune sensitization in childhood or early adulthood, and repeat exposure in sensitized individuals leads to allergic symptoms (137, 138). The most common symptom complex is allergic rhinitis, a syndrome of itchy eyes, runny nose, sneezing, fatigue, and

difficulty concentrating (139, 140). Less common but more serious is allergic asthma, a reversible airway inflammation (141). Allergic rhinitis symptoms can be managed with medications but are difficult to eliminate entirely, causing substantial morbidity and costs at the population level that are mostly related to absenteeism and presenteeism at work and school (139, 140). In severe cases, allergic asthma results in emergency department visits and hospital admissions (142–146). There appear to have been significant increases in population-level sensitization and symptomatic allergic disease over the past several decades, particularly in high-income countries and areas transitioning to industrial economies (147–150). There is also growing evidence that climate change is driving changes in pollen exposure, with significant potential impacts on human health (149, 151–154).

Information related to pollen and model exposures is important for medical and public health activities. Pollen and mold data can support the diagnosis of allergic disease and the clarification of which allergens are driving symptoms in sensitized individuals (155). Information about pollen and mold concentrations in the atmosphere, particularly forecasts, can guide medical and behavioral management in sensitized individuals, including medication timing and exposure avoidance (156). Airborne pollens and molds can be sampled and identified by specially trained individuals, and monitoring networks are established in several parts of the world. Aeroallergen monitoring is expensive, however, requiring specialized sensors and trained identifiers who can speciate pollen samples and consistently report results. As a result, aeroallergen monitoring is limited in many locations, and the data that are available are frequently not public.

Remote sensing has long held promise as a potential source for aeroallergen data (157). Both direct and indirect methods hold promise. Aeroallergens range in size from 5 to 200 μm, and their presence can be detected remotely through the air column using different methods (158). Different approaches to measuring AOD combined with ground observations have been used to estimate pollen concentrations, generally with limited discriminatory power outside periods of high pollen concentration, but recent work suggests that micropulse lidar may hold more promise (159, 160). Indirect methods using vegetation indices such as the normalized difference vegetation index (NDVI), linked with ground observations of plant phenology and aeroallergen concentrations, also hold promise, but challenges remain (161, 162). Vegetation indices are less useful for identifying phenophase in evergreen forests and can be less reliable for estimating later-season phenology for grasses and weeds and in areas with dense vegetation (163, 164). Recent advances hold promise for using vegetation indices as phenophase correlates across a range of biomes and at large scales, however, and species distribution mapping using MODIS NDVI has potential in settings meeting certain conditions (165–167).

Remote sensing of vegetation indices and weather variables, combined with ground observations and with proxy data like web searches, has great potential for modeling aeroallergen concentrations. Skilled pollen models may help improve disease management, facilitate diagnosis, and support epidemiological analyses, including analyses regarding the contribution of climate change to the changing burden of allergic disease (168, 169). In some regions, however, taking full advantage of the potential for remote sensing to better estimate aeroallergens is likely to require additional investments in ground observations.

7. CURRENT SATELLITE CAPABILITIES AND LIMITATIONS

The previous sections survey the main applications of satellite data for air quality and health and provide a variety of specific examples of satellite data and their limitations. As we conclude this review, we step back and discuss the capabilities and limitations of satellite data more broadly. Since $PM_{2.5}$ and NO_2 have emerged as the data products most widely used for satellite-based air

quality and health applications, in this section we discuss the current and future capabilities for these two pollutants in particular.

7.1. Satellite Data for Fine Particulate Matter

From the vantage point of space, satellite remote sensing can provide information on aerosol optical properties with a wide spatial coverage, a long data record, and consistent data quality. Since the early 2000s, researchers have begun exploring quantitative methods to convert satellite data such as AOD to $PM_{2.5}$ mass concentrations to cover rural and suburban populations. AOD retrieved by instruments on polar-orbiting satellites such as MODIS and VIIRS have been extensively used in various modeling frameworks to estimate daily or long-term $PM_{2.5}$ concentrations worldwide (61, 170, 171). In particular, MAIAC is an advanced algorithm providing aerosol retrievals globally twice a day at 1-km spatial resolution (172). Many studies have shown that statistical models driven by MAIAC are able to reflect daily $PM_{2.5}$ fluctuations and intraurban exposure contrasts and extend $PM_{2.5}$ exposure estimates to regions without routine ground $PM_{2.5}$ monitoring (173–175). The long data records of satellite AOD have also allowed for the estimation of historical $PM_{2.5}$ levels where regulatory air quality monitoring networks have only been established recently (176). These desirable features have facilitated research on the health effects of both acute and chronic exposure of $PM_{2.5}$ at regional to global scales (176).

A major limitation of satellite AOD products is the large proportion (on average, 50–70%) of nonrandom missing data resulting from cloud cover and high surface brightness (e.g., snow/ice cover) (177, 178). Spatial smoothing is one way to fill in the data gaps and obtain continuous $PM_{2.5}$ predictions. For example, Kloog et al. used universal kriging with daily mean $PM_{2.5}$ surfaces and random slopes to generate fully covered $PM_{2.5}$ exposure estimates (179). Simulated AOD by atmospheric CTMs have also been used as an alternative to satellite AOD in $PM_{2.5}$ prediction (180). Statistical gap–filling models have also been developed to allow for changing relationships between AOD and meteorological factors, especially cloud fraction and snow coverage. For example, Bi et al. developed an ML-based AOD gap-filling model with snow/cloud fractions and meteorological covariates that generated spatially continuous AOD data at a 1-km resolution at a daily level, with a mean validation of $R^2 > 0.9$ (181). Gap filling has been increasingly used as a routine preprocessing step in high-resolution $PM_{2.5}$ exposure modeling.

Because polar-orbiting satellites only make one or two snapshots a day over the study region, they do not capture rapidly changing air pollution events such as dust storms and wildland fires. A major advantage of the geostationary platform is its ability to observe a given region repeatedly during daytime. For example, over the United States, fire spot, smoke mask, and AOD data, as well as aerosol detection products, are available from GOES-16 every 15 min. Aerosol retrievals from geostationary satellites have been evaluated for air quality monitoring (182–184). GOES-16 AOD data have been used together with simulated $PM_{2.5}$ concentrations from backward trajectory models to assess aerosol emission sources (185). More research is needed to develop methods to fill AOD data gaps at the hourly level.

As discussed above in various examples, surface $PM_{2.5}$ from satellite data must incorporate data from ground monitors and/or model data through fusion techniques. An example of a monitor-and-satellite-fused $PM_{2.5}$ dataset is shown in **Figure 9**, which demonstrates a visualization tool for daily, 3-km surface $PM_{2.5}$ data for the entire state of California. The $PM_{2.5}$ fields are constructed by a geostatistical method that merges EPA AirNow monitor data and NASA MODIS satellite Dark Target 3-km AOD data, using a linear regression model and a surface-smoothing model based on the inverse distance weighted method (16, 186, 187). The usage of satellite data enables the generation of this type of $PM_{2.5}$ data at near real-time frequency (i.e., within 24 h of the satellite swaths), providing timely information to facilitate the decision-making of air agencies and public

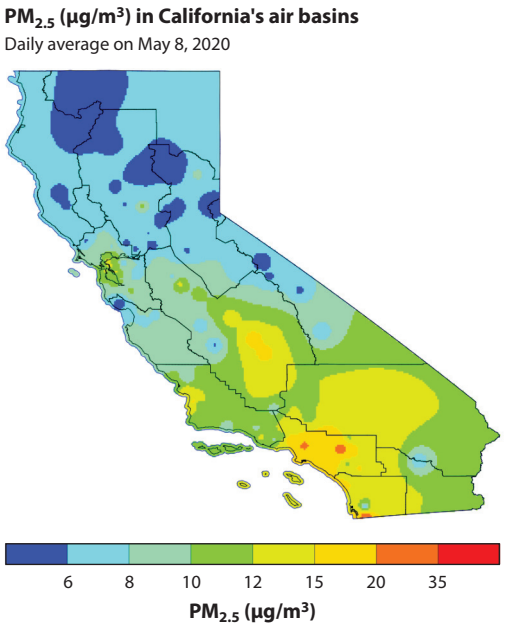

Figure 9

An example of satellite-and-monitor-fused $PM_{2.5}$ data for the entire state of California on May 8, 2020. Daily, near-real-time, 3-km $PM_{2.5}$ data were generated by the team of SJSU and NASA USRA, which are publicly accessible at the SJSU website (**http://www.met.sjsu.edu/weather/HAQAST/product2.html**). Maps and NetCDF files of previous days may be downloaded from archive (**http://www.met.sjsu.edu/~000253930/HAQAST/PM25_CALIFORNIA_DAILY/**). Figure prepared by Mohammad Al-Hamdan, Frank Freedman, and Minghui Diao. Abbreviations: NetCDF, network common data form; $PM_{2.5}$, particulate matter <2.5 µm in diameter; SJSU, San Jose State University; USRA, Universities Space Research Association.

health users. For health researchers that focus on the contiguous United States, a series of publicly available datasets have been documented (10), some of which are also available on a global basis.

To date, the overwhelming majority of satellite-driven exposure modeling has focused on $PM_{2.5}$ mass concentration. A better characterization of $PM_{2.5}$ speciation is much needed, as the spatial coverage of $PM_{2.5}$ speciation monitors is far worse than that of $PM_{2.5}$ mass monitors. Currently MISR and the future MAIA (discussed above in Section 2) offer information on aerosol type, which can be used to evaluate chemical speciation and associated health impacts.

7.2. Satellite Data for Nitrogen Dioxide

The newest satellite instruments are able to capture spatial heterogeneity in NO_2 levels between urban, suburban, and rural areas and can detect individual NO_2 emission sources such as power plants and industrial facilities (188). Satellite data from GOME2 (Global Ozone Monitoring Experiment 2) and SCIAMACHY (Scanning Imaging Absorption Spectrometer for Atmospheric Chartography) have been used together with datasets on land use characteristics to generate NO_2 exposure estimates at fine spatial scales (e.g., 100 m × 100 m) globally (54). This existing dataset is now being updated to leverage the long temporal record of OMI NO_2 column measurements and the high spatial resolution of tropospheric monitoring instrument (TROPOMI) NO_2 column measurements.

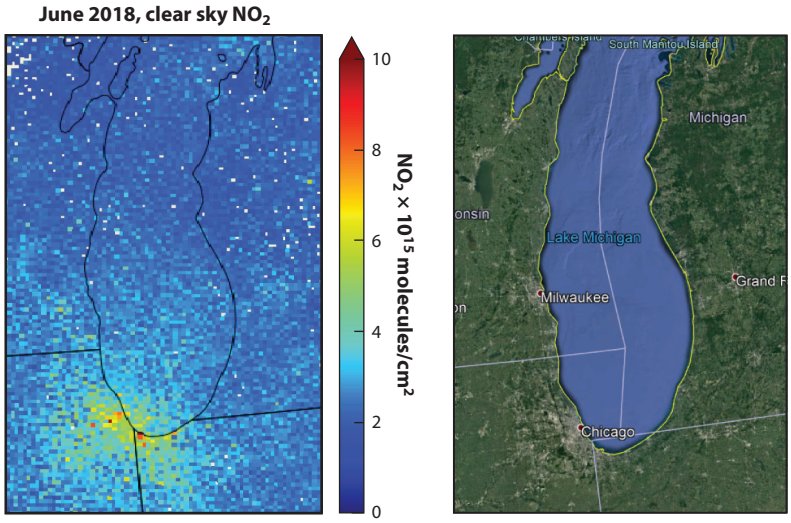

Figure 10

(*Left*) Clear sky tropospheric NO_2 columns over the Lake Michigan region aggregated onto a 4-km × 4-km grid for June 2018. (*Right*) Landsat true color image of the Lake Michigan region with major urban areas labeled. Right panel reproduced from Google Earth.

Current polar-orbiting ultraviolet–visible (UV-VIS) satellite instruments provide global, high–spatial resolution measurements of key ozone and aerosol precursor emissions at 1:00 PM local time. The TROPOMI instrument, onboard the European Space Agency's Sentinel-5 Precursor, measures key atmospheric constituents, including ozone, NO_2, SO_2, carbon monoxide (CO), methane (CH_4), and HCHO (189). TROPOMI tropospheric NO_2 retrievals have a spatial resolution of 7 × 3.5 km^2 at nadir, which allows for monitoring of urban-scale NO_x emissions on monthly timescales (190). **Figure 10** shows TROPOMI clear sky tropospheric NO_2 columns aggregated onto a 4-km × 4-km grid for June 2018. A band of high–tropospheric NO_2 columns (6–10 × 10^{15} molecules/cm^2) are observed extending from downtown Chicago, Illinois, to the southwest, as well as high–tropospheric NO_2 columns over Gary, Indiana. Elevated columns (4–6 × 10^{15} molecules/cm^2) cover the Chicago metropolitan area and extend to the east over Lake Michigan.

The future constellation of UV-VIS satellite instruments will include geostationary, daytime measurements of ozone and aerosol precursor emissions with high spatial (3–5 km) and temporal (hourly) resolution. The Korean Geostationary Environmental Monitoring Spectrometer (GEMS) will observe emissions over East Asia; it is currently in geostationary orbit and conducting on-orbit calibration and validation activities (191). NASA's Tropospheric Emissions: Monitoring of Pollution (TEMPO) will observe emissions over North America, and Europe's Sentinel-4 will observe emissions over Europe using UV-VIS-near-infrared sensors (192, 193). These new geostationary UV-VIS sensors will provide measurements with high spectral, temporal, and spatial scales for retrieving trace gas concentrations relevant to air quality.

8. CONCLUSION

Health and air quality communities have grown increasingly engaged in the utilization of satellite data, and this trend is expected to continue. New generations of satellite data, including TROPOMI, TEMPO, GEMS, and Sentinel-4, will provide higher-resolution data and, for

geostationary instruments, greater temporal coverage of select world regions. In addition to data supporting new health applications, the planned NASA MAIA mission is the first satellite launched by the United States specifically focused on health research questions. From health researchers to air quality managers and from global applications to community impacts, satellite data are transforming the way air pollution exposure is evaluated.

To discuss the opportunities for evaluating air quality with new data sources, in May 2017 the American Thoracic Society, the EPA, NASA, and the National Institute of Environmental Health Sciences convened a workshop of global experts from multiple disciplines and agencies to discuss capabilities of monitoring global air quality (2). Recommendations for research and improved data use were identified during the workshop, and it was recognized that the integration of data across monitoring technology groups is necessary to maximize the effectiveness of these technologies. Rather than viewing various monitoring technologies as competing for supremacy for use in health research, it is more constructive to realize that obtaining spatially resolved estimates of short- and long-term pollution concentrations with global spatial coverage requires combining the strengths of multiple monitoring technologies.

Despite this transformation, satellite data continue to pose challenges for new user communities. Satellite data do not provide the same information as ground monitors, and they are not always appropriate to integrate with existing analysis and decision frameworks. Rather, the appropriate use of satellite data may require a rethinking of application goals—posing questions appropriate to these novel data that would not have been possible with limited ground-based monitoring. In other cases, the utilization of satellite data is only possible through data fusion techniques with models or monitors. Unfortunately, these conceptual challenges to satellite data applications compound the practical limits facing new users of satellite data: processing new data formats, selecting among a growing inventory of instruments and retrievals, and navigating the vocabulary and acronyms common in the satellite data community.

Emerging technologies for low-cost and portable monitors are expanding the spatial coverage of monitoring data (e.g., PurpleAir), including those supporting community health analysis. However, these monitors vary in their accuracy, are not considered equivalent to traditional monitors in providing exposure data, and are still found primarily in urban areas of developed countries. Although computer models have often been used to complement ground monitors, they are limited by uncertainties in model skill and required inputs. Indeed, monitoring data are often used to evaluate and improve models, so a region with few monitors may also suffer from less reliable model data. In the context of satellite data analysis, models can play an essential role linking column values measured from space with surface pollution concentrations relevant to public health. The potential for satellite data to support public health will depend on continued development of data fusion methods to link monitors, models, and space-based observations.

The NASA HAQAST effort running from 2016 to 2020 has worked to build partnerships, develop resources, and apply research to use satellite data to improve air quality and health. In late 2020, NASA announced the next generation of this team, which will advance these goals from 2021 to 2025 (**https://haqast.org**). As the health, air quality, and remote sensing communities work together with ever-improving data sources, the role of satellite data for health exposure is expected to grow rapidly in coming years.

DISCLOSURE STATEMENT

The authors are not aware of any affiliations, memberships, funding, or financial holdings that might be perceived as affecting the objectivity of this review.

ACKNOWLEDGMENTS

Funding for this study was provided by the NASA Applied Sciences Program, with all authors supported by grants for the NASA Health and Air Quality Applied Sciences Team. A portion of this research was carried out at the Jet Propulsion Laboratory, California Institute of Technology, under contract with NASA.

LITERATURE CITED

1. Holloway T, Jacob DJ, Miller D. 2018. Short history of NASA applied science teams for air quality and health. *J. Appl. Remote Sens.* 12(4):042611
2. Cromar KR, Duncan BN, Bartonova A, Benedict K, Brauer M, et al. 2019. Air pollution monitoring for health research and patient care. An official American Thoracic Society workshop report. *Ann. Am. Thorac. Soc.* 16(10):1207–14
3. Miranda ML, Edwards SE, Keating MH, Paul CJ. 2011. Making the environmental justice grade: the relative burden of air pollution exposure in the United States. *Int. J. Environ. Res. Public Health* 8(6):1755–71
4. Martin RV, Brauer M, van Donkelaar A, Shaddick G, Narain U, Dey S. 2019. No one knows which city has the highest concentration of fine particulate matter. *Atmos. Environ. X* 3:100040
5. Shaddick G, Thomas ML, Green A, Brauer M, Donkelaar A, et al. 2018. Data integration model for air quality: a hierarchical approach to the global estimation of exposures to ambient air pollution. *J. R. Stat. Soc. C* 67(1):231–53
6. OECD (Organ. Econ. Co-op. Develop.). 2016. *The Economic Consequences of Outdoor Air Pollution.* Paris: OECD
7. de Sherbinin A, Levy MA, Zell E, Weber S, Jaiteh M. 2014. Using satellite data to develop environmental indicators. *Environ. Res. Lett.* 9:084013
8. Duncan BN, Prados AI, Lamsal LN, Liu Y, Streets DG, et al. 2014. Satellite data of atmospheric pollution for U.S. air quality applications: examples of applications, summary of data end-user resources, answers to FAQs, and common mistakes to avoid. *Atmos. Environ.* 94:647–62
9. Shaddick G, Thomas ML, Amini H, Broday D, Cohen A, et al. 2018. Data integration for the assessment of population exposure to ambient air pollution for global burden of disease assessment. *Environ. Sci. Technol.* 52(16):9069–78
10. Diao M, Holloway T, Choi S, O'Neill SM, Al-Hamdan MZ, et al. 2019. Methods, availability, and applications of $PM_{2.5}$ exposure estimates derived from ground measurements, satellite, and atmospheric models. *J. Air Waste Manag. Assoc.* 69(12):1391–414
11. Wang J, Christopher SA. 2003. Intercomparison between satellite-derived aerosol optical thickness and $PM_{2.5}$ mass: implications for air quality studies. *Geophys. Res. Lett.* 30(21):2095
12. Gupta P, Christopher SA. 2009. Particulate matter air quality assessment using integrated surface, satellite, and meteorological products: 2. A neural network approach. *J. Geophys. Res. Atmos.* 114(D20):D20205
13. Al-Hamdan MZ, Crosson WL, Limaye AS, Rickman DL, Quattrochi DA, et al. 2009. Methods for characterizing fine particulate matter using ground observations and remotely sensed data: potential use for environmental public health surveillance. *J. Air Waste Manag. Assoc.* 59(7):865–81
14. Liu Y, Franklin M, Kahn R, Koutrakis P. 2007. Using aerosol optical thickness to predict ground-level $PM_{2.5}$ concentrations in the St. Louis area: a comparison between MISR and MODIS. *Remote Sens. Environ.* 107(1):33–44
15. Paciorek CJ, Liu Y, Moreno-Macias H, Kondragunta S. 2008. Spatiotemporal associations between GOES aerosol optical depth retrievals and ground-level $PM_{2.5}$. *Environ. Sci. Technol.* 42(15):5800–6
16. Hu X, Waller LA, Lyapustin A, Wang Y, Al-Hamdan MZ, et al. 2014. Estimating ground-level $PM_{2.5}$ concentrations in the Southeastern United States using MAIAC AOD retrievals and a two-stage model. *Remote Sens. Environ.* 140:220–32
17. Ma Z, Hu X, Huang L, Bi J, Liu Y. 2014. Estimating ground-level $PM_{2.5}$ in China using satellite remote sensing. *Environ. Sci. Technol.* 48(13):7436–44

18. Zhang G, Rui X, Fan Y. 2018. Critical review of methods to estimate $PM_{2.5}$ concentrations within specified research region. *ISPRS Int. J. Geo-Inf.* 7(9):368
19. Meng X, Hand JL, Schichtel BA, Liu Y. 2018. Space-time trends of $PM_{2.5}$ constituents in the conterminous United States estimated by a machine learning approach, 2005–2015. *Environ. Int.* 121(2):1137–47
20. Bi J, Stowell J, Seto EYW, English PB, Al-Hamdan MZ, et al. 2020. Contribution of low-cost sensor measurements to the prediction of $PM_{2.5}$ levels: a case study in Imperial County, California, USA. *Environ. Res.* 180:108810
21. Hu X, Belle JH, Meng X, Wildani A, Waller LA, et al. 2017. Estimating $PM_{2.5}$ concentrations in the conterminous United States using the random forest approach. *Environ. Sci. Technol.* 51(12):6936–44
22. Liang F, Xiao Q, Huang K, Yang X, Liu F, et al. 2020. The 17-y spatiotemporal trend of $PM_{2.5}$ and its mortality burden in China. *PNAS* 117(41):25601–8
23. Meng X, Liu C, Zhang L, Wang W, Stowell J, et al. 2021. Estimating $PM_{2.5}$ concentrations in Northeastern China with full spatiotemporal coverage, 2005–2016. *Remote Sens. Environ.* 253:112203
24. Stafoggia M, Bellander T, Bucci S, Davoli M, de Hoogh K, et al. 2019. Estimation of daily PM_{10} and $PM_{2.5}$ concentrations in Italy, 2013–2015, using a spatiotemporal land-use random-forest model. *Environ. Int.* 124:170–79
25. Wang L, Bi J, Meng X, Geng G, Huang K, et al. 2020. Satellite-based assessment of the long-term efficacy of $PM_{2.5}$ pollution control policies across the Taiwan Strait. *Remote Sens. Environ.* 251:112067
26. Just A, De Carli M, Shtein A, Dorman M, Lyapustin A, Kloog I. 2018. Correcting measurement error in satellite aerosol optical depth with machine learning for modeling $PM_{2.5}$ in the Northeastern USA. *Remote Sens.* 10(5):803
27. Li T, Shen H, Yuan Q, Zhang X, Zhang L. 2017. Estimating ground-level $PM_{2.5}$ by fusing satellite and station observations: a geo-intelligent deep learning approach: deep learning for $PM_{2.5}$ estimation. *Geophys. Res. Lett.* 44(23):11985–93
28. Park Y, Kwon B, Heo J, Hu X, Liu Y, Moon T. 2020. Estimating $PM_{2.5}$ concentration of the conterminous United States via interpretable convolutional neural networks. *Environ. Pollut.* 256:113395
29. Li L, Girguis M, Lurmann F, Pavlovic N, McClure C, et al. 2020. Ensemble-based deep learning for estimating $PM_{2.5}$ over California with multisource big data including wildfire smoke. *Environ. Int.* 145:106143
30. Xiao Q, Chang HH, Geng G, Liu Y. 2018. An ensemble machine-learning model to predict historical $PM_{2.5}$ concentrations in China from satellite data. *Environ. Sci. Technol.* 52(22):13260–69
31. Jin X, Fiore AM, Civerolo K, Bi J, Liu Y, et al. 2019. Comparison of multiple $PM_{2.5}$ exposure products for estimating health benefits of emission controls over New York State, USA. *Environ. Res. Lett.* 14(8):084023
32. Kelly JT, Jang C, Timin B, Di Q, Schwartz J, et al. 2020. Examining $PM_{2.5}$ concentrations and exposure using multiple models. *Environ. Res.* In press. **https://doi.org/10.1016/j.envres.2020.110432**
33. Berrocal VJ, Guan Y, Muyskens A, Wang H, Reich BJ, et al. 2020. A comparison of statistical and machine learning methods for creating national daily maps of ambient $PM_{2.5}$ concentration. *Atmos. Environ.* 222:117130
34. Snider G, Weagle CL, Murdymootoo KK, Ring A, Ritchie Y, et al. 2016. Variation in global chemical composition of $PM_{2.5}$: emerging results from SPARTAN. *Atmospheric Chem. Phys.* 16(15):9629–53
35. Crumeyrolle S, Chen G, Ziemba L, Beyersdorf A, Thornhill L, et al. 2014. Factors that influence surface $PM_{2.5}$ values inferred from satellite observations: perspective gained for the US Baltimore–Washington metropolitan area during DISCOVER-AQ. *Atmos. Chem. Phys.* 14(4):2139–53
36. Streets DG, Canty T, Carmichael GR, de Foy B, Dickerson RR, et al. 2013. Emissions estimation from satellite retrievals: a review of current capability. *Atmos. Environ.* 77:1011–42
37. Strickland MJ, Hao H, Hu X, Chang HH, Darrow LA, Liu Y. 2016. Pediatric emergency visits and short-term changes in $PM_{2.5}$ concentrations in the U.S. state of Georgia. *Environ. Health Perspect.* 124(5):690–96
38. Stowell JD, Geng G, Saikawa E, Chang HH, Fu J, et al. 2019. Associations of wildfire smoke $PM_{2.5}$ exposure with cardiorespiratory events in Colorado 2011–2014. *Environ. Int.* 133(Pt. A):105151

39. Geng G, Murray NL, Tong D, Fu JS, Hu X, et al. 2018. Satellite-based daily $PM_{2.5}$ estimates during fire seasons in Colorado. *J. Geophys. Res. Atmos.* 123(15):8159–71
40. Xiao Q, Chen H, Strickland MJ, Kan H, Chang HH, et al. 2018. Associations between birth outcomes and maternal $PM_{2.5}$ exposure in Shanghai: a comparison of three exposure assessment approaches. *Environ. Int.* 117:226–36
41. Di Q, Dai L, Wang Y, Zanobetti A, Choirat C, et al. 2017. Association of short-term exposure to air pollution with mortality in older adults. *JAMA* 318(24):2446
42. Huang K, Liang F, Yang X, Liu F, Li J, et al. 2019. Long term exposure to ambient fine particulate matter and incidence of stroke: prospective cohort study from the China-PAR project. *BMJ* 367:l6720
43. Liang F, Liu F, Huang K, Yang X, Li J, et al. 2020. Long-term exposure to fine particulate matter and cardiovascular disease in China. *J. Am. Coll. Cardiol.* 75(7):707–17
44. Tapia VL, Vasquez BV, Vu B, Liu Y, Steenland K, Gonzales GF. 2020. Association between maternal exposure to particulate matter ($PM_{2.5}$) and adverse pregnancy outcomes in Lima, Peru. *J. Expo. Sci. Environ. Epidemiol.* 30(4):689–97
45. Tapia V, Steenland K, Sarnat SE, Vu B, Liu Y, et al. 2020. Time-series analysis of ambient $PM_{2.5}$ and cardiorespiratory emergency room visits in Lima, Peru during 2010–2016. *J. Expo. Sci. Environ. Epidemiol.* 30(4):680–88
46. Tapia V, Steenland K, Vu B, Liu Y, Vásquez V, Gonzales GF. 2020. $PM2_{.5}$ exposure on daily cardiorespiratory mortality in Lima, Peru, from 2010 to 2016. *Environ. Health Glob. Access Sci. Source* 19(1):63
47. Heft-Neal S, Burney J, Bendavid E, Burke M. 2018. Robust relationship between air quality and infant mortality in Africa. *Nature* 559(7713):254–58
48. Khreis H, Kelly C, Tate J, Parslow R, Lucas K, Nieuwenhuijsen M. 2017. Exposure to traffic-related air pollution and risk of development of childhood asthma: a systematic review and meta-analysis. *Environ. Int.* 100:1–31
49. Lamsal LN, Duncan BN, Yoshida Y, Krotkov NA, Pickering KE, et al. 2015. U.S. NO2 trends (2005–2013): EPA Air Quality System (AQS) data versus improved observations from the Ozone Monitoring Instrument (OMI). *Atmos. Environ.* 110:130–43
50. Cooper MJ, Martin RV, McLinden CA, Brook JR. 2020. Inferring ground-level nitrogen dioxide concentrations at fine spatial resolution applied to the TROPOMI satellite instrument. *Environ. Res. Lett.* 15(10):104013
51. Richmond-Bryant J, Owen RC, Graham S, Snyder M, McDow S, et al. 2017. Estimation of on-road NO_2 concentrations, NO_2/NO_X ratios, and related roadway gradients from near-road monitoring data. *Air Qual. Atmos. Health* 10(5):611–25
52. Anderson HR, Favarato G, Atkinson RW. 2013. Erratum to: Long-term exposure to air pollution and the incidence of asthma: meta-analysis of cohort studies. *Air Qual. Atmos. Health* 6(2):541–42
53. HEI (Health Effects Inst.). 2010. *Traffic-related air pollution: a critical review of the literature on emissions, exposure, and health effects*. Spec. Rep. 17, HEI, Boston
54. Larkin A, Geddes JA, Martin RV, Xiao Q, Liu Y, et al. 2017. Global land use regression model for nitrogen dioxide air pollution. *Environ. Sci. Technol.* 51(12):6957–64
55. Franklin M, Kalashnikova OV, Garay MJ. 2017. Size-resolved particulate matter concentrations derived from 4.4 km-resolution size-fractionated Multi-angle Imaging SpectroRadiometer (MISR) aerosol optical depth over Southern California. *Remote Sens. Environ.* 196:312–23
56. Geng G, Meng X, He K, Liu Y. 2020. Random forest models for $PM_{2.5}$ speciation concentrations using MISR fractional AODs. *Environ. Res. Lett.* 15(3):034056
57. Liu Y, Koutrakis P, Kahn R. 2007. Estimating fine particulate matter component concentrations and size distributions using satellite-retrieved fractional aerosol optical depth: part 1—method development. *J. Air Waste Manag. Assoc.* 57(11):1351–59
58. Liu Y, Koutrakis P, Kahn R, Turquety S, Yantosca RM. 2007. Estimating fine particulate matter component concentrations and size distributions using satellite-retrieved fractional aerosol optical depth: part 2—a case study. *J. Air Waste Manag. Assoc.* 57(11):1360–69

59. Diner DJ, Boland SW, Brauer M, Bruegge C, Burke KA, et al. 2018. Advances in multiangle satellite remote sensing of speciated airborne particulate matter and association with adverse health effects: from MISR to MAIA. *J. Appl. Remote Sens.* 12(4):042603
60. Liu Y, Diner DJ. 2017. Multi-angle imager for aerosols: a satellite investigation to benefit public health. *Public Health Rep.* 132(1):14–17
61. van Donkelaar A, Martin RV, Brauer M, Kahn R, Levy R, et al. 2010. Global estimates of ambient fine particulate matter concentrations from satellite-based aerosol optical depth: development and application. *Environ. Health Perspect.* 118(6):847–55
62. Evans J, van Donkelaar A, Martin RV, Burnett R, Rainham DG, et al. 2013. Estimates of global mortality attributable to particulate air pollution using satellite imagery. *Environ. Res.* 120:33–42
63. Cohen AJ, Brauer M, Burnett R, Anderson HR, Frostad J, et al. 2017. Estimates and 25-year trends of the global burden of disease attributable to ambient air pollution: an analysis of data from the Global Burden of Diseases Study 2015. *Lancet* 389(10082):1907–18
64. Malley CS, Kuylenstierna JCI, Vallack HW, Henze DK, Blencowe H, Ashmore MR. 2017. Preterm birth associated with maternal fine particulate matter exposure: a global, regional and national assessment. *Environ. Int.* 101:173–82
65. Anenberg SC, Miller J, Minjares R, Du L, Henze DK, et al. 2017. Impacts and mitigation of excess diesel-related NO*x* emissions in 11 major vehicle markets. *Nature* 545(7655):467–71
66. Anenberg SC, Miller J, Henze DK, Minjares R, Achakulwisut P. 2019. The global burden of transportation tailpipe emissions on air pollution-related mortality in 2010 and 2015. *Environ. Res. Lett.* 14(9):094012
67. Lacey FG, Henze DK, Lee CJ, van Donkelaar A, Martin RV. 2017. Transient climate and ambient health impacts due to national solid fuel cookstove emissions. *PNAS* 114(6):1269–74
68. Brauer M, Freedman G, Frostad J, van Donkelaar A, Martin RV, et al. 2016. Ambient air pollution exposure estimation for the global burden of disease 2013. *Environ. Sci. Technol.* 50(1):79–88
69. van Donkelaar A, Martin RV, Brauer M, Hsu NC, Kahn RA, et al. 2016. Global estimates of fine particulate matter using a combined geophysical-statistical method with information from satellites, models, and monitors. *Environ. Sci. Technol.* 50(7):3762–72
70. Stanaway JD, Afshin A, Gakidou E, Lim SS, Abate D, et al. 2018. Global, regional, and national comparative risk assessment of 84 behavioural, environmental and occupational, and metabolic risks or clusters of risks for 195 countries and territories, 1990–2017: a systematic analysis for the Global Burden of Disease Study 2017. *Lancet* 392(10159):1923–94
71. Burnett RT, Pope CA, Ezzati M, Olives C, Lim SS, et al. 2014. An integrated risk function for estimating the global burden of disease attributable to ambient fine particulate matter exposure. *Environ. Health Perspect.* 122(4):397–403
72. Yin P, Brauer M, Cohen A, Burnett RT, Liu J, et al. 2017. Long-term fine particulate matter exposure and nonaccidental and cause-specific mortality in a large national cohort of Chinese men. *Environ. Health Perspect.* 125(11):117002
73. Li T, Zhang Y, Wang J, Xu D, Yin Z, et al. 2018. All-cause mortality risk associated with long-term exposure to ambient $PM_{2.5}$ in China: a cohort study. *Lancet Public Health* 3(10):e470–77
74. U.N. Environ. Assem. 2014. *Resolutions and decisions adopted by the United Nations Environment Assembly of the United Nations Environment Programme at its first session on 27 June 2014*. Tech. Rep., U.N., Geneva. **https://www.unep.org/resources/report/resolutions-and-decisions-adopted-united-nations-environment-assembly-united**
75. World Health Assem. 68. 2015. *Health and the environment: addressing the health impact of air pollution: draft resolution proposed by the delegations of Albania, Chile, Colombia, France, Germany, Monaco, Norway, Panama, Sweden, Switzerland, Ukraine, United States of America, Uruguay and Zambia*. Tech. Rep. A68/A/CONF./2 Rev.1, World Health Organ., Geneva
76. Li M, Klimont Z, Zhang Q, Martin RV, Zheng B, et al. 2018. Comparison and evaluation of anthropogenic emissions of SO_2 and NO_X over China. *Atmos. Chem. Phys.* 18(5):3433–56
77. Zheng B, Tong D, Li M, Liu F, Hong C, et al. 2018. Trends in China's anthropogenic emissions since 2010 as the consequence of clean air actions. *Atmos. Chem. Phys.* 18(19):14095–111

78. Ciarelli G, Colette A, Schucht S, Beekmann M, Andersson C, et al. 2019. Long-term health impact assessment of total $PM_{2.5}$ in Europe during the 1990–2015 period. *Atmos. Environ. X* 3:100032
79. Liousse C, Assamoi E, Criqui P, Granier C, Rosset R. 2014. Explosive growth in African combustion emissions from 2005 to 2030. *Environ. Res. Lett.* 9(3):035003
80. Achakulwisut P, Brauer M, Hystad P, Anenberg SC. 2019. Global, national, and urban burdens of paediatric asthma incidence attributable to ambient NO_2 pollution: estimates from global datasets. *Lancet Planet. Health* 3(4):e166–78
81. Zhang Y, Cooper OR, Gaudel A, Thompson AM, Nédélec P, et al. 2016. Tropospheric ozone change from 1980 to 2010 dominated by equatorward redistribution of emissions. *Nat. Geosci.* 9(12):875–79
82. Duncan BN, Lamsal LN, Thompson AM, Yoshida Y, Lu Z, et al. 2016. A space-based, high-resolution view of notable changes in urban NO_x pollution around the world (2005–2014). *J. Geophys. Res. Atmos.* 121(2):976–96
83. Li C, McLinden C, Fioletov V, Krotkov N, Carn S, et al. 2017. India is overtaking China as the world's largest emitter of anthropogenic sulfur dioxide. *Sci. Rep.* 7:14304
84. Montgomery A, Holloway T. 2018. Assessing the relationship between satellite-derived NO_2 and economic growth over the 100 most populous global cities. *J. Appl. Remote Sens.* 12(4):042607
85. Bauwens M, Compernolle S, Stavrakou T, Muller JF, van Gent J, et al. 2020. Impact of coronavirus outbreak on NO_2 pollution assessed using TROPOMI and OMI observations. *Geophys. Res. Lett.* 47(11):e2020GL087978
86. Verstraeten WW, Neu JL, Williams JE, Bowman KW, Worden JR, Boersma KF. 2015. Rapid increases in tropospheric ozone production and export from China. *Nat. Geosci.* 8(9):690–95
87. Puchalski MA, Walker JT, Beachley GM, Zondlo MA, Benedict KB, et al. 2019. Need for improved monitoring of spatial and temporal trends of reduced nitrogen. *EM Mag. Environ. Manag.* 2019(July): 7–10
88. Wang R, Guo X, Pan D, Kelly JT, Bash JO, et al. 2020. Monthly patterns of ammonia over the contiguous United States at 2-km resolution. *Geophys. Res. Lett.* 48(5):e2020GL090579
89. Zhu L, Jacob DJ, Kim PS, Fisher JA, Yu K, et al. 2016. Observing atmospheric formaldehyde (HCHO) from space: validation and intercomparison of six retrievals from four satellites (OMI, GOME2A, GOME2B, OMPS) with SEAC4RS aircraft observations over the southeast US. *Atmos. Chem. Phys.* 16(21):13477–90
90. Fu D, Millet DB, Wells KC, Payne VH, Yu S, et al. 2019. Direct retrieval of isoprene from satellite-based infrared measurements. *Nat. Commun.* 10(1):3811
91. EPA (Environ. Protect. Agency). 2020. *Our nation's air*. Tech. Rep., EPA, Washington, DC
92. TCEQ (Texas Comm. Environ. Qual.). 2016. *Houston-Galveston-Brazoria attainment demonstration State Implementation Plan revision for the 2008 eight-hour ozone standard nonattainment area*. Proj. Number 2016-016-SIP-NR, TCEQ, Austin, TX
93. Conn. Dep. Energy Environ. Protect. 2017. *Enclosure A: revision to Connecticut's state implementation plan: 8-hour ozone attainment demonstration for the Connecticut portion of the New York-northern New Jersey-Long Island (NY-NJ-CT) nonattainment area*. Tech. Support Doc., Connect. Dep. Energy Environ. Protect., Hartford, CT
94. Conn. Dep. Energy Environ. Protect. 2017. *Enclosure A : revision to Connecticut's state implementation plan: 8-hour ozone attainment demonstration for the greater Connecticut nonattainment area*. Tech. Support Doc., Connect. Dep. Energy Environ. Protect., Hartford, CT
95. Geigert M. 2018. *Guide to using satellite images in support of exceptional event demonstrations*. Tech. Guid. Doc. 2, NASA Health Air Qual. Appl. Sci. Team, Washington, DC
96. Fiore AM, Pierce R, Dickerson R, Lin M. 2014. Detecting and attributing episodic high background ozone events. *EM Mag. Environ. Manag.* 2014(Feb.):22–28
97. Kahn R. 2020. A global perspective on wildfires. *Eos*, Jan. 27. **https://eos.org/science-updates/a-global-perspective-on-wildfires**
98. Ryan KC, Knapp EE, Varner JM. 2013. Prescribed fire in North American forests and woodlands: history, current practice, and challenges. *Front. Ecol. Environ.* 11(S1):e15–24

99. Reid CE, Brauer M, Johnston FH, Jerrett M, Balmes JR, Elliott CT. 2016. Critical review of health impacts of wildfire smoke exposure. *Environ. Health Perspect.* 124(9):1334–43
100. Larsen AE, Reich BJ, Ruminski M, Rappold AG. 2018. Impacts of fire smoke plumes on regional air quality, 2006–2013. *J. Expo. Sci. Environ. Epidemiol.* 28(4):319–27
101. Fann N, Alman B, Broome RA, Morgan GG, Johnston FH, et al. 2018. The health impacts and economic value of wildland fire episodes in the U.S.: 2008–2012. *Sci. Total Environ.* 610–611:802–9
102. Jaffe DA, O'Neill SM, Larkin NK, Holder AL, Peterson DL, et al. 2020. Wildfire and prescribed burning impacts on air quality in the United States. *J. Air Waste Manag. Assoc.* 70(6):583–615
103. Hu Y, Odman MT, Chang ME, Jackson W, Lee S, et al. 2008. Simulation of air quality impacts from prescribed fires on an urban area. *Environ. Sci. Technol.* 42(10):3676–82
104. DA Jaffe, Wigder NL. 2012. Ozone production from wildfires: a critical review. *Atmos. Environ.* 51:1–10
105. Conn. Dep. Energy Environ. Protect. 2017. *May 2016 ozone exceptional event analysis*. Tech. Support Doc., Conn. Dep. Energy Environ. Protect., Hartford, CT
106. Chen J, Vaughan J, Avise J, O'Neill S, Lamb B. 2008. Enhancement and evaluation of the AIRPACT ozone and $PM_{2.5}$ forecast system for the Pacific Northwest. *J. Geophys. Res. Atmos.* 113(D14):D14305
107. Larkin NK, O'Neill SM, Solomon R, Raffuse S, Strand T, et al. 2009. The BlueSky smoke modeling framework. *Int. J. Wildland Fire* 18(8):906–20
108. Chen J, Anderson K, Pavlovic R, Moran MD, Englefield P, et al. 2019. The FireWork v2.0 air quality forecast system with biomass burning emissions from the Canadian Forest Fire Emissions Prediction System v2.03. *Geosci. Model. Dev.* 12(7):3283–310
109. Grell G, Freitas SR, Stuefer M, Fast J. 2011. Inclusion of biomass burning in WRF-Chem: impact of wildfires on weather forecasts. *Atmos. Chem. Phys.* 11(11):5289–303
110. Lee P, McQueen J, Stajner I, Huang J, Pan L, et al. 2017. NAQFC developmental forecast guidance for fine particulate matter ($PM_{2.5}$). *Weather Forecast* 32(1):343–60
111. Odman OT, Huang R, Pophale AA, Sakhpara RD, Hu Y, et al. 2018. Forecasting the impacts of prescribed fires for dynamic air quality management. *Atmosphere* 9(6):220
112. Ichoku C, Ellison L. 2014. Global top-down smoke-aerosol emissions estimation using satellite fire radiative power measurements. *Atmos. Chem. Phys.* 14(13):6643–67
113. Sofiev M, Ermakova T, Vankevich R. 2012. Evaluation of the smoke-injection height from wild-land fires using remote-sensing data. *Atmos. Chem. Phys.* 12(4):1995–2006
114. Li F, Zhang X, Roy DP, Kondragunta S. 2019. Estimation of biomass-burning emissions by fusing the fire radiative power retrievals from polar-orbiting and geostationary satellites across the conterminous United States. *Atmos. Environ.* 211:274–87
115. Cleland SE, West JJ, Jia Y, Reid S, Raffuse S, et al. 2020. Estimating wildfire smoke concentrations during the October 2017 California fires through BME space/time data fusion of observed, modeled, and satellite-derived $PM_{2.5}$. *Environ. Sci. Technol.* 54(21):13439–47
116. Hunt W, Winker D, Vaughan M, Powell K, Lucker P, Weimer C. 2009. CALIPSO lidar description and performance assessment. *J. Atmos. Ocean. Technol.* 26:1214–28
117. Diner D, Beckert J, Reilly TH, Bruegge C, Conel JE, et al. 1998. Multi-angle Imaging SpectroRadiometer (MISR) instrument description and experiment overview. *IEEE Trans. Geosci. Remote Sens.* 36:1072–87
118. Lyapustin A, Wang Y, Korkin S, Kahn R, Winker D. 2020. MAIAC thermal technique for smoke injection height from MODIS. *IEEE Geosci. Remote Sens. Lett.* 17(5):730–34
119. Marsha A, Larkin NK. 2019. A statistical model for predicting $PM_{2.5}$ for the western United States. *J. Air Waste Manag. Assoc.* 69(10):1215–29
120. Tian D, Wang Y, Bergin M, Hu Y, Liu Y, Russell AG. 2008. Air quality impacts from prescribed forest fires under different management practices. *Environ. Sci. Technol.* 42(8):2767–72
121. Sarnat JA, Marmur A, Klein M, Kim E, Russell AG, et al. 2008. Fine particle sources and cardiorespiratory morbidity: an application of chemical mass balance and factor analytical source-apportionment methods. *Environ. Health Perspect.* 116(4):459–66
122. Bates JT, Weber RJ, Abrams J, Verma V, Fang T, et al. 2015. Reactive oxygen species generation linked to sources of atmospheric particulate matter and cardiorespiratory effects. *Environ. Sci. Technol.* 49(22):13605–12

123. Bates JT, Fang T, Verma V, Zeng L, Weber RJ, et al. 2019. Review of acellular assays of ambient particulate matter oxidative potential: methods and relationships with composition, sources, and health effects. *Environ. Sci. Technol.* 53(8):4003–19
124. Hu Y, Ai HH, Odman MT, Vaidyanathan A, Russell AG. 2019. Development of a WebGIS-based analysis tool for human health protection from the impacts of prescribed fire smoke in Southeastern USA. *Int. J. Environ. Res. Public Health* 16(11):1981
125. Huang R, Hu Y, Russell AG, Mulholland JA, Odman MT. 2019. The impacts of prescribed fire on $PM_{2.5}$ air quality and human health: application to asthma-related emergency room visits in Georgia, USA. *Int. J. Environ. Res. Public Health* 16(13):2312–12
126. Johnson Gaither C, Afrin S, Garcia-Menendez F, Odman MT, Huang R, et al. 2019. African American exposure to prescribed fire smoke in Georgia, USA. *Int. J. Environ. Res. Public Health* 16(17):3079
127. Crooks JL, Cascio WE, Percy MS, Reyes J, Neas LM, Hilborn ED. 2016. The association between dust storms and daily non-accidental mortality in the United States, 1993–2005. *Environ. Health Perspect.* 124(11):1735–43
128. Rice MB, Mittleman MA. 2017. Dust storms, heart attacks, and protecting those at risk. *Eur. Heart J.* 38(43):3209–10
129. García-Pando CP, Stanton MC, Diggle PJ, Trzaska S, Miller RL, et al. 2014. Soil dust aerosols and wind as predictors of seasonal meningitis incidence in Niger. *Environ. Health Perspect.* 122(7):679–86
130. Tong DQ, Wang JXL, Gill TE, Lei H, Wang B. 2017. Intensified dust storm activity and Valley fever infection in the southwestern United States. *Geophys. Res. Lett.* 44(9):4304–12
131. Tong DQ, Dan M, Wang T, Lee P. 2012. Long-term dust climatology in the western United States reconstructed from routine aerosol ground monitoring. *Atmos. Chem. Phys.* 12(11):5189–205
132. Prospero JM, Ginoux P, Torres O, Nicholson SE, Gill TE. 2002. Environmental characterization of global sources of atmospheric soil dust identified with the Nimbus 7 Total Ozone Mapping Spectrometer (TOMS) absorbing aerosol product. *Rev. Geophys.* 40(1):2–31
133. Rivera Rivera NI, Gill TE, Bleiweiss MP, Hand JL. 2010. Source characteristics of hazardous Chihuahuan Desert dust outbreaks. *Atmos. Environ.* 44(20):2457–68
134. Baddock MC, Gill TE, Bullard JE, Acosta MD, Rivera NIR. 2011. Geomorphology of the Chihuahuan Desert based on potential dust emissions. *J. Maps* 7(1):249–59
135. Lee JA, Gill TE, Mulligan KR, Dominguez Acosta M, Perez AE. 2009. Land use/land cover and point sources of the 15 December 2003 dust storm in southwestern North America. *Geomorphology* 105(1):18–27
136. Ginoux P, Prospero JM, Gill TE, Hsu NC, Zhao M. 2012. Global-scale attribution of anthropogenic and natural dust sources and their emission rates based on MODIS Deep Blue aerosol products. *Rev. Geophys.* 50(3):1–36
137. Warm K, Hedman L, Lindberg A, Lötvall J, Lundbäck B, Rönmark E. 2015. Allergic sensitization is age-dependently associated with rhinitis, but less so with asthma. *J. Allergy Clin. Immunol.* 136(6):1559–65.e2
138. Bartra J, Mullol J, del Cuvillo A, Dávila I, Ferrer M, et al. 2007. Air pollution and allergens. *J. Investig. Allergol. Clin. Immunol.* 17(Suppl. 2):3–8
139. Linneberg A, Dam Petersen K, Hahn-Pedersen J, Hammerby E, Serup-Hansen N, Boxall N. 2016. Burden of allergic respiratory disease: a systematic review. *Clin. Mol. Allergy* 14(1):12
140. Steinsvaag SK. 2012. Allergic rhinitis: an updated overview. *Curr. Allergy Asthma Rep.* 12(2):99–103
141. Cockcroft DW. 1983. Mechanism of perennial allergic asthma. *Lancet* 322(8344):253–56
142. Darrow LA, Hess J, Rogers CA, Tolbert PE, Klein M, Sarnat SE. 2012. Ambient pollen concentrations and emergency department visits for asthma and wheeze. *J. Allergy Clin. Immunol.* 130(3):630–38.e4
143. Erbas B, Akram M, Dharmage SC, Tham R, Dennekamp M, et al. 2012. The role of seasonal grass pollen on childhood asthma emergency department presentations. *Clin. Exp. Allergy* 42(5):799–805
144. Erbas B, Jazayeri M, Lambert KA, Katelaris CH, Prendergast LA, et al. 2018. Outdoor pollen is a trigger of child and adolescent asthma emergency department presentations: a systematic review and meta-analysis. *Allergy* 73(8):1632–41
145. Erbas B, Chang J-H, Dharmage S, Ong EK, Hyndman R, et al. 2007. Do levels of airborne grass pollen influence asthma hospital admissions? *Clin. Exp. Allergy* 37(11):1641–47

146. Im W, Schneider D. 2005. Effect of weed pollen on children's hospital admissions for asthma during the fall season. *Arch. Environ. Occup. Health* 60(5):257–65
147. Chen C-H, Xirasagar S, Lin H-C. 2006. Seasonality in adult asthma admissions, air pollutant levels, and climate: a population-based study. *J. Asthma* 43(4):287–92
148. D'Amato G. 2002. Environmental urban factors (air pollution and allergens) and the rising trends in allergic respiratory diseases. *Allergy* 57(S72):30–33
149. Shea KM, Truckner RT, Weber RW, Peden DB. 2008. Climate change and allergic disease. *J. Allergy Clin. Immunol.* 122(3):443–53
150. Zanolin ME, Pattaro C, Corsico A, Bugiani M, Carrozzi L, et al. 2004. The role of climate on the geographic variability of asthma, allergic rhinitis and respiratory symptoms: results from the Italian study of asthma in young adults. *Allergy* 59(3):306–14
151. Hamaoui-Laguel L, Vautard R, Liu L, Solmon F, Viovy N, et al. 2015. Effects of climate change and seed dispersal on airborne ragweed pollen loads in Europe. *Nat. Clim. Change* 5(8):766–71
152. Lake IR, Jones NR, Agnew M, Goodess CM, Giorgi F, et al. 2017. Climate change and future pollen allergy in Europe. *Environ. Health Perspect.* 125(3):385–91
153. Neumann JE, Anenberg SC, Weinberger KR, Amend M, Gulati S, et al. 2019. Estimates of present and future asthma emergency department visits associated with exposure to oak, birch, and grass pollen in the United States. *GeoHealth* 3(1):11–27
154. Zhang Y, Isukapalli SS, Bielory L, Georgopoulos PG. 2013. Bayesian analysis of climate change effects on observed and projected airborne levels of birch pollen. *Atmos. Environ.* 68:64–73
155. Barber D, de la Torre F, Feo F, Florido F, Guardia P, et al. 2008. Understanding patient sensitization profiles in complex pollen areas: a molecular epidemiological study. *Allergy* 63(11):1550–58
156. Kmenta M, Zetter R, Berger U, Bastl K. 2016. Pollen information consumption as an indicator of pollen allergy burden. *Wien. klin. Wochenschr.* 128(1–2):59–67
157. Skjøth CA, Šikoparija B, Jäger S, EAN-Netw. 2013. Pollen sources. In *Allergenic Pollen*, ed. M Sofiev, K-C Bergmann, pp. 9–27. Dordrecht, Neth.: Springer
158. Scheifinger H, Belmonte J, Buters J, Celenk S, Damialis A, et al. 2013. Monitoring, modelling and forecasting of the pollen season. In *Allergenic Pollen*, ed. M Sofiev, K-C Bergmann, pp. 71–126. Dordrecht, Neth.: Springer
159. Noh YM, Lee H, Mueller D, Lee K, Shin D, et al. 2013. Investigation of the diurnal pattern of the vertical distribution of pollen in the lower troposphere using LIDAR. *Atmos. Chem. Phys.* 13(15):7619–29
160. Sicard M, Izquierdo R, Alarcón M, Belmonte J, Comerón A, Baldasano JM. 2016. Near-surface and columnar measurements with a micro pulse lidar of atmospheric pollen in Barcelona, Spain. *Atmos. Chem. Phys.* 16(11):6805–21
161. González-Naharro R, Quirós E, Fernández-Rodríguez S, Silva-Palacios I, Maya-Manzano JM, et al. 2019. Relationship of NDVI and oak (*Quercus*) pollen including a predictive model in the SW Mediterranean region. *Sci. Total Environ.* 676:407–19
162. Hogda KA, Karlsen SR, Solheim I, Tommervik H, Ramfjord H. 2002. The start dates of birch pollen seasons in Fennoscandia studied by NOAA AVHRR NDVI data. In *Proceedings of the IEEE International Geoscience and Remote Sensing Symposium*. New York: IEEE
163. Hmimina G, Dufrêne E, Pontailler J-Y, Delpierre N, Aubinet M, et al. 2013. Evaluation of the potential of MODIS satellite data to predict vegetation phenology in different biomes: an investigation using ground-based NDVI measurements. *Remote Sens. Environ.* 132:145–58
164. Butterfield HS, Malmström CM. 2009. The effects of phenology on indirect measures of aboveground biomass in annual grasses. *Int. J. Remote Sens.* 30(12):3133–46
165. Soudani K, Hmimina G, Delpierre N, Pontailler J-Y, Aubinet M, et al. 2012. Ground-based network of NDVI measurements for tracking temporal dynamics of canopy structure and vegetation phenology in different biomes. *Remote Sens. Environ.* 123:234–45
166. Yan E, Wang G, Lin H, Xia C, Sun H. 2015. Phenology-based classification of vegetation cover types in Northeast China using MODIS NDVI and EVI time series. *Int. J. Remote Sens.* 36(2):489–512
167. Feilhauer H, He KS, Rocchini D. 2012. Modeling species distribution using niche-based proxies derived from composite bioclimatic variables and MODIS NDVI. *Remote Sens.* 4(7):2057–75

168. Devadas R, Huete AR, Vicendese D, Erbas B, Beggs PJ, et al. 2018. Dynamic ecological observations from satellites inform aerobiology of allergenic grass pollen. *Sci. Total Environ.* 633:441–51
169. Hall J, Lo F, Saha S, Vaidyanathan A, Hess J. 2020. Internet searches offer insight into early-season pollen patterns in observation-free zones. *Sci. Rep.* 10:11334
170. Kloog I, Chudnovsky AA, Just AC, Nordio F, Koutrakis P, et al. 2014. A new hybrid spatio-temporal model for estimating daily multi-year $PM_{2.5}$ concentrations across northeastern USA using high resolution aerosol optical depth data. *Atmos. Environ.* 95:581–90
171. Xiao Q, Chang HH, Geng G, Liu Y. 2018. An ensemble machine-learning model to predict historical $PM_{2.5}$ concentrations in China from satellite data. *Environ. Sci. Technol.* 52(22):13260–69
172. Lyapustin A, Wang Y, Korkin S, Huang D. 2018. MODIS Collection 6 MAIAC algorithm. *Atmos. Meas. Tech.* 11(10):5741–65
173. Chudnovsky AA, Kostinski A, Lyapustin A, Koutrakis P. 2013. Spatial scales of pollution from variable resolution satellite imaging. *Environ. Pollut.* 172:131–38
174. Liang F, Xiao Q, Wang Y, Lyapustin A, Li G, et al. 2018. MAIAC-based long-term spatiotemporal trends of $PM_{2.5}$ in Beijing, China. *Sci. Total Environ.* 616–17:1589–98
175. Vu BN, Sánchez O, Bi J, Xiao Q, Hansel NN, et al. 2019. Developing an advanced $PM_{2.5}$ exposure model in Lima, Peru. *Remote Sens.* 11(6):641
176. Ma Z, Hu X, Sayer AM, Levy R, Zhang Q, et al. 2016. Satellite-based spatiotemporal trends in $PM^{2.5}$ concentrations: China, 2004–2013. *Environ. Health Perspect.* 124(2):184–92
177. Belle JH, Chang HH, Wang Y, Hu X, Lyapustin A, Liu Y. 2017. The potential impact of satellite-retrieved cloud parameters on ground-level $PM_{2.5}$ mass and composition. *Int. J. Environ. Res. Public Health* 14(10):1244
178. Belle JH, Liu Y. 2016. Evaluation of aqua MODIS collection 6 AOD parameters for air quality research over the continental United States. *Remote Sens.* 8(10):815
179. Kloog I, Koutrakis P, Coull BA, Lee HJ, Schwartz J. 2011. Assessing temporally and spatially resolved $PM_{2.5}$ exposures for epidemiological studies using satellite aerosol optical depth measurements. *Atmos. Environ.* 45(35):6267–75
180. Di Q, Koutrakis P, Schwartz J. 2016. A hybrid prediction model for $PM_{2.5}$ mass and components using a chemical transport model and land use regression. *Atmos. Environ.* 131:390–99
181. Bi J, Belle JH, Wang Y, Lyapustin AI, Wildani A, Liu Y. 2019. Impacts of snow and cloud covers on satellite-derived $PM_{2.5}$ levels. *Remote Sens. Environ.* 221:665–74
182. Choi M, Kim J, Lee J, Kim M, Park Y-J, et al. 2016. GOCI Yonsei Aerosol Retrieval (YAER) algorithm and validation during the DRAGON-NE Asia 2012 campaign. *Atmos. Meas. Tech.* 9(3):1377–98
183. Liu Y, Paciorek CJ, Koutrakis P. 2009. Estimating regional spatial and temporal variability of $PM_{2.5}$ concentrations using satellite data, meteorology, and land use information. *Environ. Health Perspect.* 117(6):886–92
184. Xu J-W, Martin R, Donkelaar A, Kim J, Choi M, et al. 2015. Estimating ground-level $PM_{2.5}$ in Eastern China using aerosol optical depth determined from the GOCI Satellite Instrument. *Atmos. Chem. Phys.* 15:13133–44
185. Nizar S, Dodamani BM. 2020. Satellite-based top-down Lagrangian approach to quantify aerosol emissions over California. *Q. J. R. Meteorol. Soc.* 146(729):1626–35
186. Al-Hamdan MZ, Crosson WL, Limaye AS, Rickman DL, Quattrochi DA, et al. 2009. Methods for characterizing fine particulate matter using ground observations and remotely sensed data: potential use for environmental public health surveillance. *J. Air Waste Manag. Assoc.* 59(7):865–81
187. Al-Hamdan MZ, Crosson WL, Economou SA, Estes MGJ, Estes SM, et al. 2014. Environmental public health applications using remotely sensed data. *Geocarto Int.* 29(1):85–98
188. Goldberg DL, Lu Z, Streets DG, de Foy B, Griffin D, et al. 2019. Enhanced capabilities of TROPOMI NO_2: estimating NO*X* from North American cities and power plants. *Environ. Sci. Technol.* 53(21):12594–601
189. Veefkind JP, Aben I, McMullan K, Förster H, de Vries J, et al. 2012. TROPOMI on the ESA Sentinel-5 Precursor: a GMES mission for global observations of the atmospheric composition for climate, air quality and ozone layer applications. *Remote Sens. Environ.* 120:70–83

190. Eskes H, van Geffen J, Sneep M, Apituley A, Veefkind JP. 2019. *Sentinel-5 precursor/TROPOMI level 2 product user manual nitrogendioxide*. User Manual, R. Neth. Meteorol. Inst., De Bilt, Neth.
191. Kim J, Kim M, Choi M. 2017. Monitoring aerosol properties in East Asia from geostationary orbit: GOCI, MI and GEMS. In *Air Pollution in Eastern Asia: An Integrated Perspective*, ed. I Bouarar, X Wang, GP Brasseur, pp. 323–33. Cham, Switz.: Springer Int.
192. Zoogman P, Liu X, Suleiman RM, Pennington WF, Flittner DE, et al. 2017. Tropospheric emissions: monitoring of pollution (TEMPO). *J. Quant. Spectrosc. Radiat. Transf.* 186:17–39
193. Ingmann P, Veihelmann B, Langen J, Lamarre D, Stark H, Courrèges-Lacoste GB. 2012. Requirements for the GMES Atmosphere Service and ESA's implementation concept: Sentinels-4/-5 and -5p. *Remote Sens. Environ.* 120:58–69

Annual Review of Biomedical Data Science

Volume 4, 2021

Contents

Errata

An online log of corrections to *Annual Review of Biomedical Data Science* articles may be found at http://www.annualreviews.org/errata/biodatasci